

RESEARCH MEMORANDUM

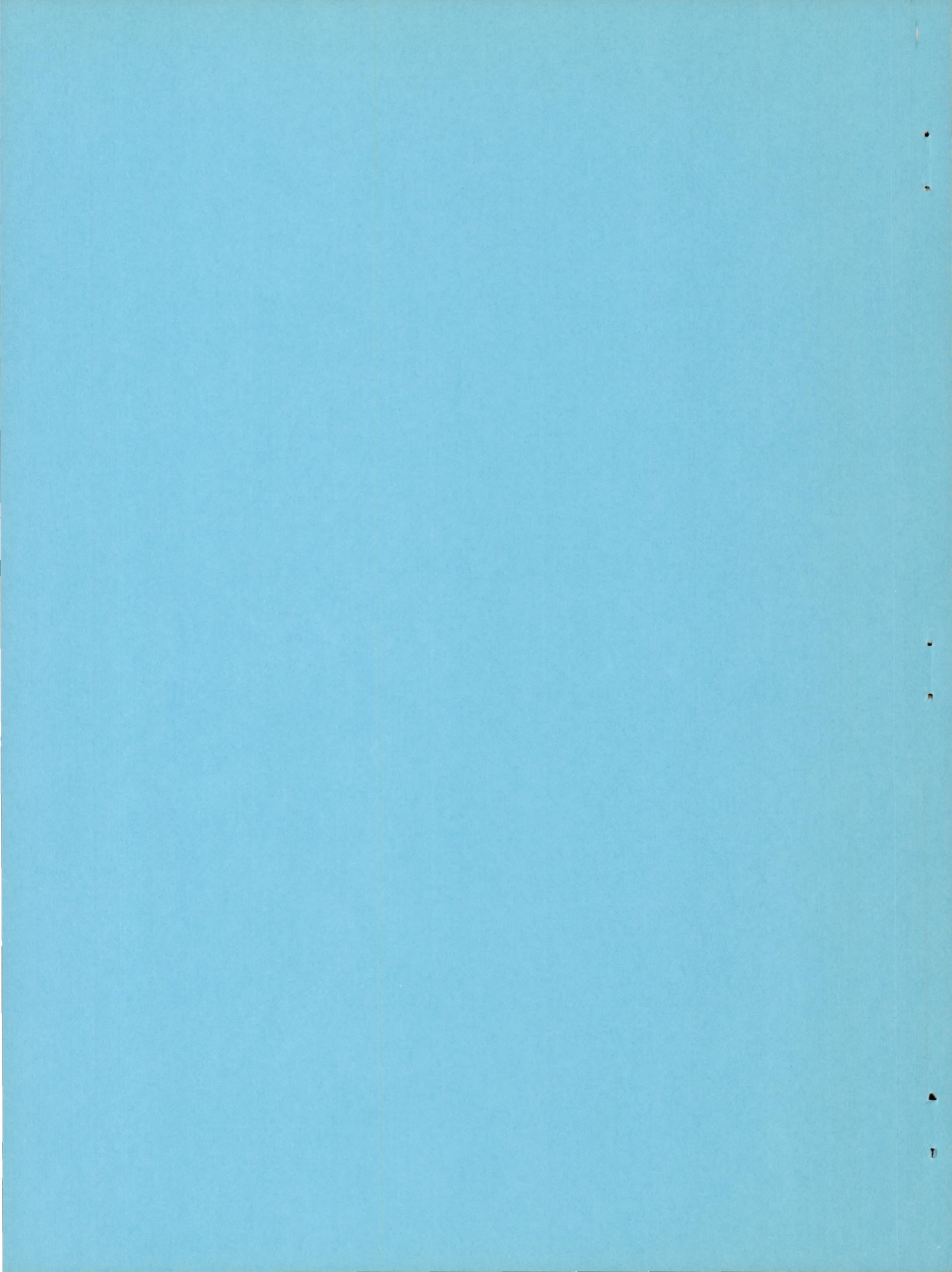
INVESTIGATION OF THE AERODYNAMIC EFFECTS OF AN EXTERNAL
STORE IN COMBINATION WITH 60° DELTA AND LOW-ASPECT-
RATIO TAPERED WINGS AT A MACH NUMBER OF 1.9

By Ellery B. May, Jr.

Langley Aeronautical Laboratory
Langley Field, Va.

NATIONAL ADVISORY COMMITTEE
FOR AERONAUTICS
WASHINGTON

January 9, 1951
Declassified November 8, 1957



NATIONAL ADVISORY COMMITTEE FOR AERONAUTICS

RESEARCH MEMORANDUM

INVESTIGATION OF THE AERODYNAMIC EFFECTS OF AN EXTERNAL
STORE IN COMBINATION WITH 60° DELTA AND LOW-ASPECT-
RATIO TAPERED WINGS AT A MACH NUMBER OF 1.9

By Ellery B. May, Jr.

SUMMARY

A wind-tunnel investigation was made of an external store of fineness ratio 8.6 which was located on the chord plane of several low-aspect-ratio wings. The work was carried out at a Mach number of 1.9 on wings having 60° leading-edge sweepback and unswept trailing edges with taper ratios of 0 and 0.28 and on an unswept wing having a taper ratio of 0.625. The test Reynolds numbers ranged between 2.3×10^6 and 4.0×10^6 .

Locating the store so that the nose was behind the wing leading edge appeared to be the most important factor in minimizing drag for store installations on a sweptback wing. No conclusions can be made regarding the optimum position of the store with the nose behind the leading edge since only one such configuration was investigated. With the store nose ahead of the wing leading edge, moving the store outboard or rearward caused a small reduction in drag. In most cases the lift-curve slope was increased about in proportion to the increase in area. With the store located adjacent to the outer wing panel a loading breakdown obtained between the store, the inner wing panel, and the outer wing panel of one wing showed no noticeable interference effects on drag at low angles of attack. At the higher angles of attack, trends indicate that favorable interference effects on drag probably exist. Adding the store adjacent to control surfaces had little effect on control characteristics.

INTRODUCTION

The extremely thin, high-density wings favored for use on high-speed aircraft oftentimes limit the space available for the storage of such items as fuel, armament, and radar equipment. Readily accessible,

fixed, or droppable external stores attached to the wings of such aircraft offer a practical means of increasing their storage capacity. Suitable shapes and locations of external stores have been developed which minimize adverse effects on an airplane's aerodynamic characteristics at subsonic and transonic speeds (references 1 and 2), but little work has been done at supersonic speeds. Accordingly, the brief experimental investigation reported herein was carried out on one particular external store at a Mach number of 1.9 in the Langley 9- by 12-inch supersonic blowdown tunnel. The body shape investigated is believed representative of stores currently under consideration and its interference effects might also be considered representative of those produced by a cold ram-jet power unit.

The store was a body of revolution of fineness ratio 8.6 having its axis located in a streamwise direction of the wing chord plane. The work was carried out on wings having 60° leading-edge sweepback and unswept trailing edges with taper ratios of 0 and 0.28, and on an unswept wing having a taper ratio of 0.625. An investigation was made to determine the effects of store position on the aerodynamic characteristics of the wing, the loading breakdown between the store and the inner and the outer wing panels, and the effects of the store on the characteristics of several control-surface arrangements.

COEFFICIENTS AND SYMBOLS

The following coefficients are presented about the wind axes of the model:

C_L lift coefficient $\left(\frac{\text{Lift}}{qS}\right)$

C_D drag coefficient $\left(\frac{\text{Drag}}{qS}\right)$

C_m pitching-moment coefficient $\left(\frac{\text{Pitching moment}}{qS\bar{c}}\right)$

$C_{l_{\text{gross}}}$ gross rolling-moment coefficient
 $\left(\frac{\text{Wing-panel rolling moment}}{2qSb}\right)$

$C_{n_{gross}}$	gross yawing-moment coefficient $\left(\frac{\text{Wing-panel yawing moment}}{2qSb} \right)$
C_l	rolling-moment coefficient $(C_{l_{gross}} - C_{l_{gross}(\delta=0^\circ)})$
C_n	yawing-moment coefficient $(C_{n_{gross}} - C_{n_{gross}(\delta=0^\circ)})$
$\Delta C_L, \Delta C_D, \Delta C_m,$ and so forth	increment in coefficient due to control-surface deflection or addition of store

The following coefficients are presented about the tip control-surface axes of the model.

C_{N_f}	control-surface normal-force coefficient $\left(\frac{N_f}{qS_f} \right)$
C_{m_f}	control-surface pitching-moment coefficient $\left(\frac{M_f}{qS_f \bar{c}_f} \right)$
N_f	control-surface normal force
M_f	control-surface pitching moment (hinge moment about control-surface pivot axis)
q	free-stream dynamic pressure
S	exposed semispan wing area, square inches
S_f	control-surface area (one control)
c	local chord
c_r	chord of wing at wing-fuselage juncture
\bar{c}	wing mean aerodynamic chord
\bar{c}_f	control-surface mean aerodynamic chord
b	wing span (twice distance from fuselage axis to wing tip)

b_f	control-surface span
α	angle of attack measured with respect to free-stream direction
δ	control-surface deflection measured with respect to wing chord plane
R	Reynolds number based on mean aerodynamic chord of exposed wing area
M	Mach number

Subscripts:

α	slope of curve of coefficient plotted against angle of attack $\left(\frac{dC_L}{d\alpha}, \frac{dC_l}{d\alpha}, \text{ and so forth} \right)$
δ	slope of curve of coefficient plotted against control-surface deflection $\left(\frac{dC_L}{d\delta}, \frac{dC_l}{d\delta}, \text{ and so forth} \right)$

DESCRIPTION OF MODELS

Photographs of the wing models are shown as figure 1. The external store and its principal dimensions are shown in figure 2. The three semispan models and their principal dimensions are shown in figures 3 to 5.

The external store was a body of revolution with a fineness ratio of 8.6. For all conditions the store was mounted on the wing chord plane with the store axis parallel to the model plane of symmetry. On wing model 1, the store was located at several spanwise and chordwise positions (fig. 3). The store position on model 2 was approximately the same as position 1 on model 1. On wing model 3, the store was located adjacent to the outboard end of the control with the store midchord point at 0.50c.

Wing model 1 (fig. 3) and wing model 2 (fig. 4) were semispan models of 60° delta wings of aspect ratio 2.3. Model 1 had a constant-chord trailing-edge control which extended from the wing-fuselage juncture to the store juncture at $0.62b/2$. Model 2 (described in detail in reference 3) had a full-chord tip control which comprised the outer one-third of the exposed wing semispan. With the tip removed, the value of the

aspect ratio was reduced to 1.3 and the value of the taper ratio was increased to 0.28. Wing model 3 (fig. 5) was a semispan model of an unswept wing of aspect ratio 2.5 and a taper ratio of 0.625 (described in detail in reference 4). The wing had a 0.25c trailing-edge control which extended from $0.45b/2$ to $0.70b/2$.

TUNNEL AND TEST TECHNIQUE

The Langley 9- by 12-inch supersonic blowdown tunnel is a nonreturn-type tunnel, utilizing the exhaust air from the Langley 19-foot pressure tunnel. The air enters at an absolute pressure of about $2\frac{1}{3}$ atmospheres and contains about 0.3 percent of water by weight.

The model arrangements are similar to those reported in references 3 and 4. The semispan models are cantilevered from a five-component strain-gage balance mounted flush with the tunnel wall. The balance and fuselage rotate with the wing as the angle of attack is changed. The forces and moments are measured with respect to the balance axes and are rotated and transferred to the wind axes of the model. The semispan models are tested in the presence of, but not attached to, a half-fuselage which is shimmed out 0.25 inch from the tunnel wall to minimize wall boundary-layer effects. A 0.02-inch clearance gap existed between the wing and the fuselage. Further discussion of the test technique is reported in references 4 and 5.

In addition to measuring the forces and moments on the complete wings with and without the store, the forces and moments acting on the tip control in the presence of the inner wing with and without the store and on the store in the presence of the inner wing of model 2 were measured. This technique was accomplished by transmitting the loads to the balance by means of a mounting staff extending through a hollowed-out portion of the inner wing panel. A more detailed explanation of this test arrangement can be found in reference 3.

The dynamic pressure and test Reynolds number decreased about 5 percent during the course of each run because of the decreased pressure of the inlet air. The average dynamic pressure was 11.5 pounds per square inch. The average Reynolds numbers, based on the mean aerodynamic chords, were 4.0×10^6 for models 1 and 2 and 2.3×10^6 for model 3. The average Reynolds number of the store, based on its length, was 4.8×10^6 .

ACCURACY OF DATA

Free-stream Mach number has been calibrated at 1.90 ± 0.02 . Calibration tests, which were made with the model removed, indicated that the static pressure varied about ± 1.5 percent from a mean value for the region normally occupied by the wing. A discussion is given in reference 5 of the various factors which might influence the test results, such as humidity effects and methods of mounting.

No tare corrections have been applied to any of the data presented. In some instances small errors in fabrication and model setup caused asymmetrical conditions. (These conditions are indicated in the lift and pitching-moment data of figs. 12 and 13.) These slightly asymmetrical conditions would not, however, affect the value of the data for comparative purposes. The magnitude of random errors that existed, based on the accuracy of the measuring and recording equipment and fluctuations of the air stream, are believed to be of the following order:

Wings		Tip control and store	
Variable	Error	Variable	Error
α	$\pm 0.05^\circ$	C_L	± 0.002
δ	.20°	C_D	.001
C_L	.003	C_m	.001
C_D	.0005	$C_{L_{gross}}$.0002
C_m	.001	$C_{N_{gross}}$.0002
$C_{L_{gross}}$.0004	C_{N_f}	.005
$C_{N_{gross}}$.0003	C_{m_f}	.008

Misalignment between the wing chord plane and the fuselage axis was less than $\pm 0.05^\circ$ for all of the configurations. Static calibration indicated no measurable change in control-surface deflection caused by control-surface loading.

RESULTS AND DISCUSSION

Loading Breakdown

Figure 6 presents the test data of the loading breakdown on a 60° swept-wing configuration (model 2) consisting of an outboard and an inboard wing panel and of an external store at one location (fig. 4). All data of figure 6 were reduced to coefficient form using the constants of the complete wing geometry to allow analysis of the data on a common basis. The data showed that adding the store did not affect the loading on the outer wing panel. Therefore, in figure 6, because of the large number of test arrangements considered, data for the outer wing panel are presented for only the store-on condition. Some lift and drag characteristics are listed in the following table to better illustrate the division of loading between the various components of the model. In interpreting the results of this table, it should be pointed out that addition of the store blanketed about 10 percent of the exposed wing area.

Configurations	Description	$C_{L\alpha}$	C_D ($\alpha = 0^\circ$)
1	Store in presence of inner wing panel	0.004	0.007
2	Outer wing panel in presence of inner wing panel	.006	.003
3	Outer wing panel in presence of inner wing panel with store	.006	.003
4	Inner wing panel	.031	.012
5	Inner wing panel with store	.032	.019
6	Complete wing	.039	.014
7	Complete wing with store	.040	.021

Adding the store at the outboard and rearward position to either the inner wing panel or the complete wing caused a large increase in the drag coefficient, as can be seen by examination of the tabulated characteristics for configurations 4, 5, 6, and 7. At zero angle of

attack this increase equaled the measured drag coefficient of the store in the presence of the inner wing panel; this result indicated no interference effect on drag. At higher angles of attack trends would indicate that favorable interference effects on drag probably exist, since the increment in drag between the store-off and the store-on configuration increased at a slower rate than did the drag of the store in the presence of the inner wing panel (fig. 6).

Adding the store increased the lift-curve slope of both the inner wing panel and the complete wing by 0.001. From an examination of the data of configurations 1, 4, and 5, it appears that this increase was proportional to the overhanging area of the store and that the lift carried on the remaining portion of the store was about the same as the lift normally carried on the wing area which was blanketed by the store. The loads on the outer wing panel were not affected by addition of the store adjacent to it on the inner wing panel.

Store Position

Drag effects.- Test data for model 1 with the store at various locations are presented in figure 7. Drag increments caused by addition of the store as obtained from these data have been summarized in figure 8. The store nose was located behind the wing leading edge for position 2 and ahead for positions 1, 3, and 4. At positions 1 and 4, the store nose was the same distance ahead of the wing leading edge. Also presented in figure 8 for comparative purposes is the drag-coefficient increment caused by adding the store to model 3 as obtained from the data of figures 9 and 10 (but based on the wing area of model 1).

At zero lift coefficient, with the store nose ahead of the wing leading edge, moving the store inboard (from position 3 to 4) increased the value of the drag coefficient approximately 0.0015 (fig. 8); while moving the store rearward (from position 3 to 1) decreased the value of the drag coefficient approximately 0.001. Inboard or rearward store movements which moved the store nose from ahead of to behind the wing leading edge (from positions 1 to 2 and 4 to 2) decreased the values of the coefficient approximately 0.002 and 0.0045, respectively. The substantially lower values of drag for this condition indicate the importance of keeping the store nose behind the wing leading edge. The range of configurations tested did not permit the determination of the effects of store location for the condition of the store nose behind the wing leading edge.

When the lift coefficient was increased to 0.3, the store drag-coefficient increment was decreased to 0.003 for the inboard and

rearward position, making such a store location doubly attractive. For the inboard and forward location (position 4) the increment increased substantially and for both outboard locations increased slightly.

The increase in drag coefficient at zero lift caused by adding the store to the basic wing ranged from 0.0045 for the inboard and rearward position to 0.009 for the inboard and forward position as compared with a calculated value of store-alone pressure drag coefficient of 0.0075 using the method of characteristics in an undisturbed flow field.

Effects on pitching moment and lift.- Figure 2 lists the store center-of-gravity location for each store position. Adding the store in either of the forward positions (fig. 7) shifted the model center of pressure forward about 2 percent of the wing mean aerodynamic chord, while adding the store in either of the rearward positions shifted the model center of pressure rearward about 1 percent of the wing mean aerodynamic chord. Adding the store at positions 1, 2, and 3 increased the lift-curve slope up to 5 percent in about the same proportion as the increase in area (fig. 7). Adding the store at position 4, however, decreased the lift-curve slope slightly.

Effect of Store on Control Characteristics

Figures 9 to 16 present basic test data for determining the effects of the store on control characteristics. Loads measured on the tip control alone (figs. 15 and 16) are presented with respect to the tip axes and were reduced to coefficient form using the tip control-surface geometry. Cross plots of these data at constant angle of attack are presented in figures 17 to 19. In some instances the results are compared with theory. The methods used for calculating the flap characteristics are described in references 6 and 7.

Adding a store to the wings adjacent to the control surfaces had little effect on the control characteristics for all of the three combinations investigated (figs. 17 to 19). It is interesting to note that, with equal control-surface areas and with stores off, (fig. 18) the experimental rolling-moment effectiveness of the trailing-edge control on the delta wing was only about one-half the effectiveness of the tip control on the delta wing. The theoretical rolling-moment effectiveness of the trailing-edge control would be only about one-third of the theoretical rolling moment of the tip control. However, about 95 percent of the theoretical value was realized for the trailing-edge control, whereas only about 70 percent was realized for the tip control.

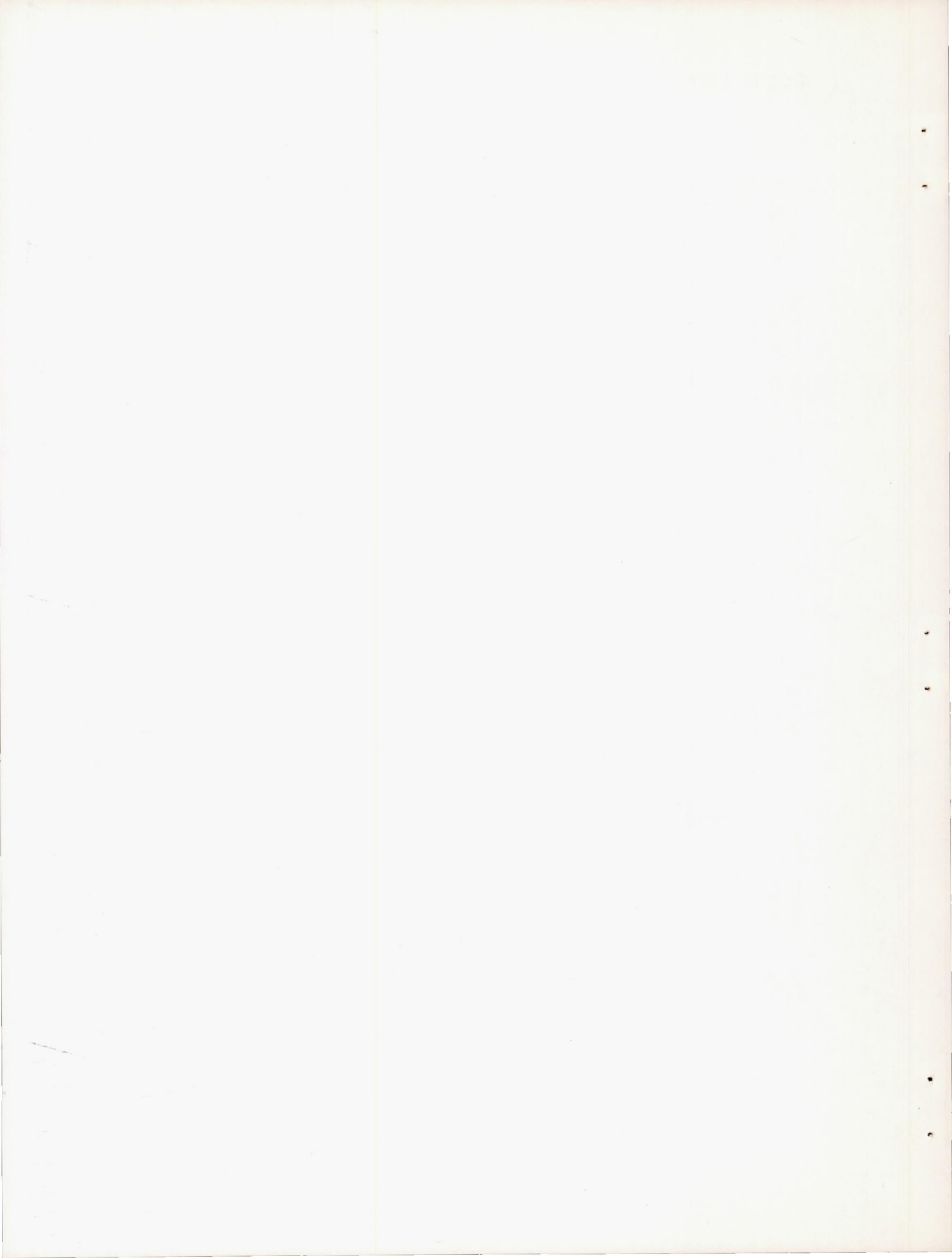
CONCLUDING REMARKS

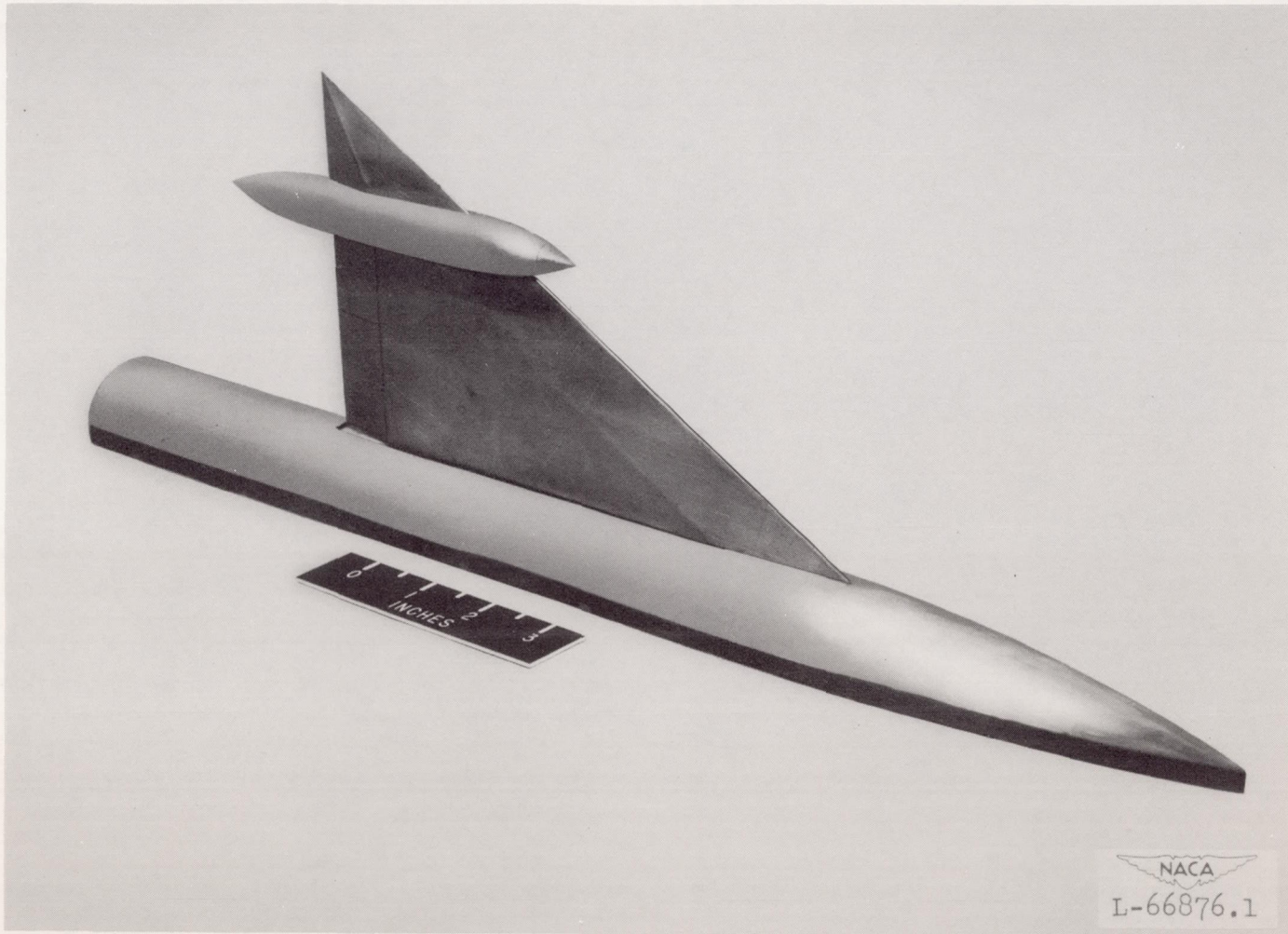
An investigation has been carried out at a Mach number of 1.9 on one particular external store tested in conjunction with several wings. It appeared that in positioning the store on a sweptback wing having a subsonic leading edge the most important factor in minimizing drag effects was to locate the store nose behind the wing leading edge. No conclusions can be made regarding the optimum position of the store with the nose behind the leading edge since only one such configuration was investigated. With the store nose ahead of the wing leading edge, moving the store outboard or rearward caused a small reduction in drag. For most store positions, the lift-curve slope was increased about in proportion to the increase in area. From a loading breakdown investigation, adding the store adjacent to the outer wing panel on a sweptback wing caused no noticeable interference effects on drag at low angles of attack. At higher angles of attack, trends indicate that favorable interference effects on drag probably exist. Adding the store adjacent to control surfaces had little effect on the control characteristics.

Langley Aeronautical Laboratory
National Advisory Committee for Aeronautics
Langley Field, Va.

REFERENCES

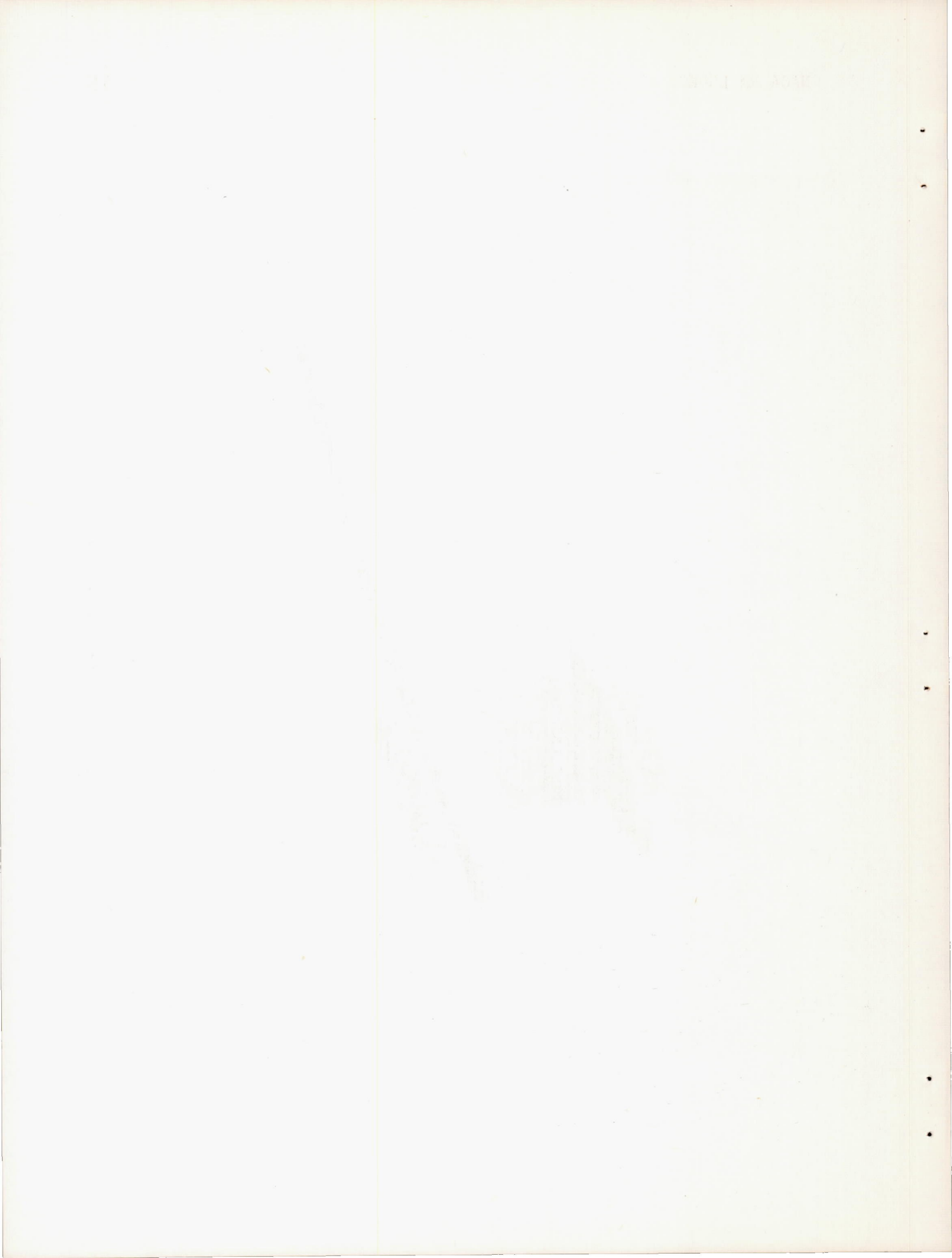
1. Silvers, H. Norman, and Spreemann, Kenneth P.: Experimental Investigation of Various External-Store Configurations on a Model of a Tailless Airplane with a Sweptback Wing. NACA RM L9K25, 1950.
2. Silvers, H. Norman, and Spreemann, Kenneth P.: Wind-Tunnel Investigation of a Wing-Fuselage Combination with External Stores. NACA RM L7K20, 1948.
3. Conner, D. William, and May, Ellery B., Jr.: Control Effectiveness Load and Hinge-Moment Characteristics of a Tip Control Surface on a Delta Wing at a Mach Number of 1.9. NACA RM L9H05, 1949.
4. Mitchell, Meade H., Jr.: Effects of Varying the Size and Location of Trailing-Edge Flap-Type Controls on the Aerodynamic Characteristics of an Unswept Wing at a Mach Number of 1.9. NACA RM L50F08, 1950.
5. Conner, D. William: Aerodynamic Characteristics of Two All-Movable Wings Tested in the Presence of a Fuselage at a Mach Number of 1.9. NACA RM L8H04, 1948.
6. Lagerstrom, P. A., and Graham, Martha E.: Linearized Theory of Supersonic Control Surfaces. Jour. Aero. Sci., vol. 16, no. 1, Jan. 1949, pp. 31-34.
7. Lagerstrom, P. A., Wall, D., and Graham, M. E.: Formulas in Three-Dimensional Wing Theory. Rep. No. SM-11901, Douglas Aircraft Co., Inc., July 8, 1946.

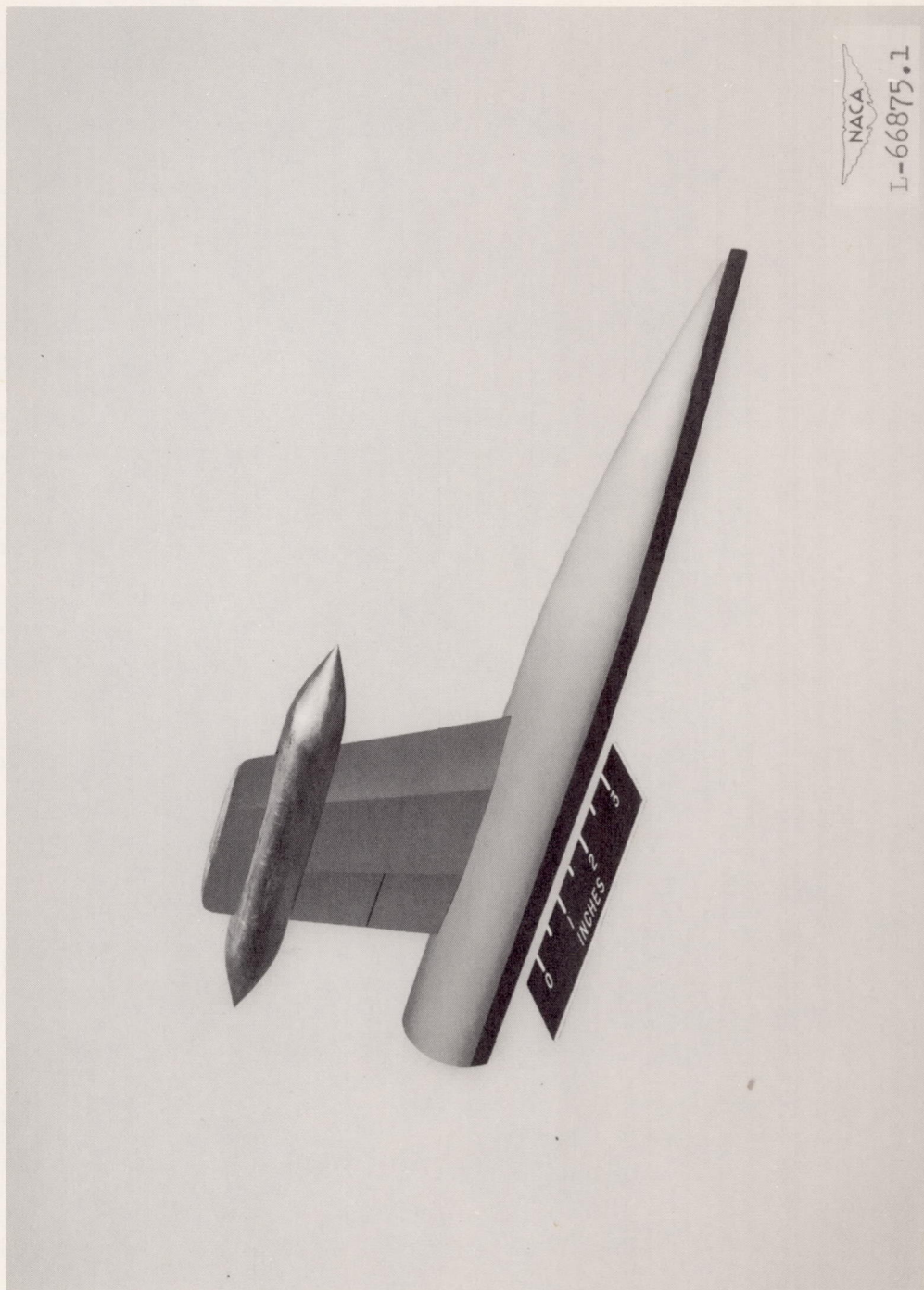




(a) Model 1 with store in position 1.

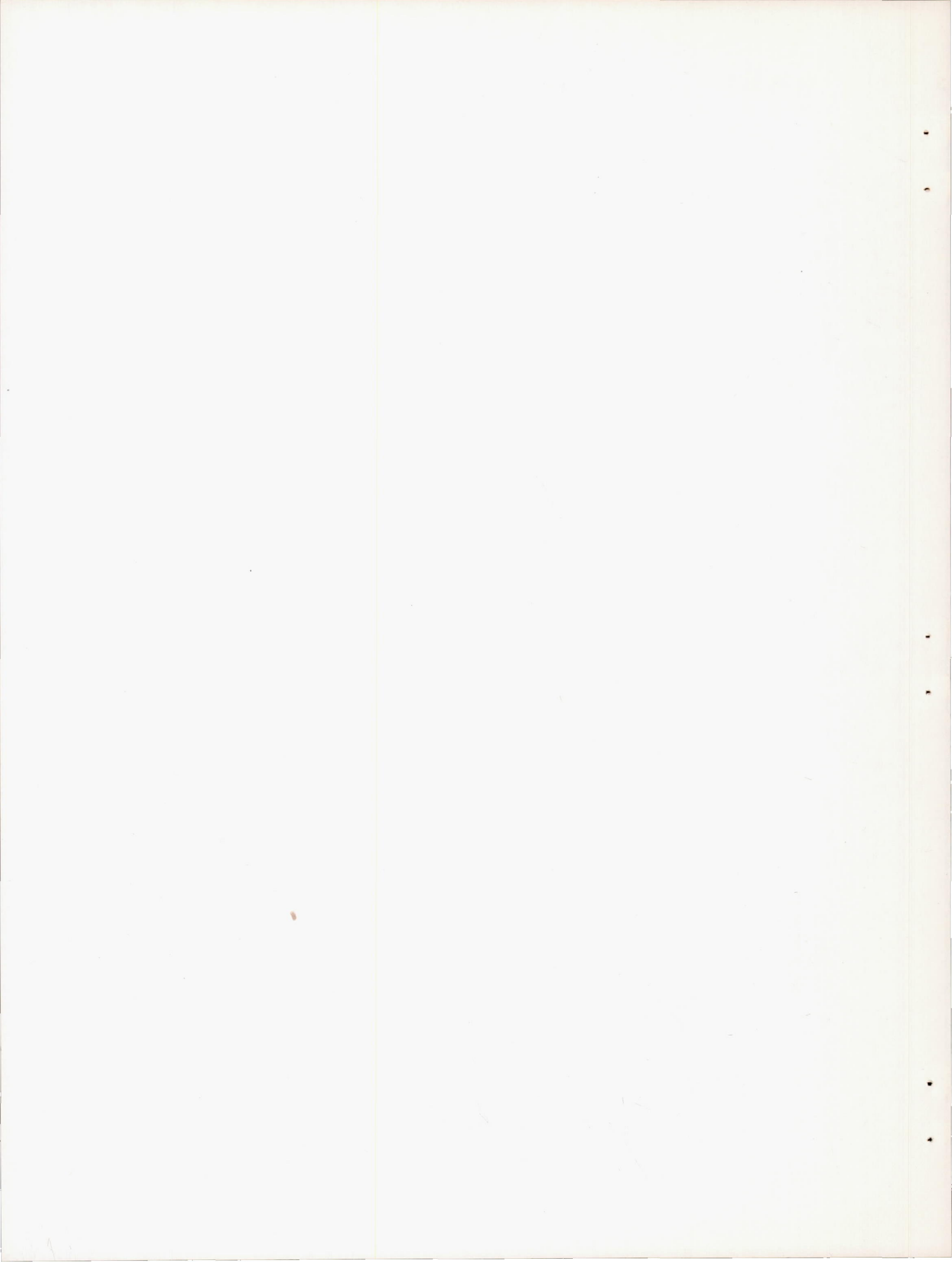
Figure 1.- Photographs of models used in the investigation.

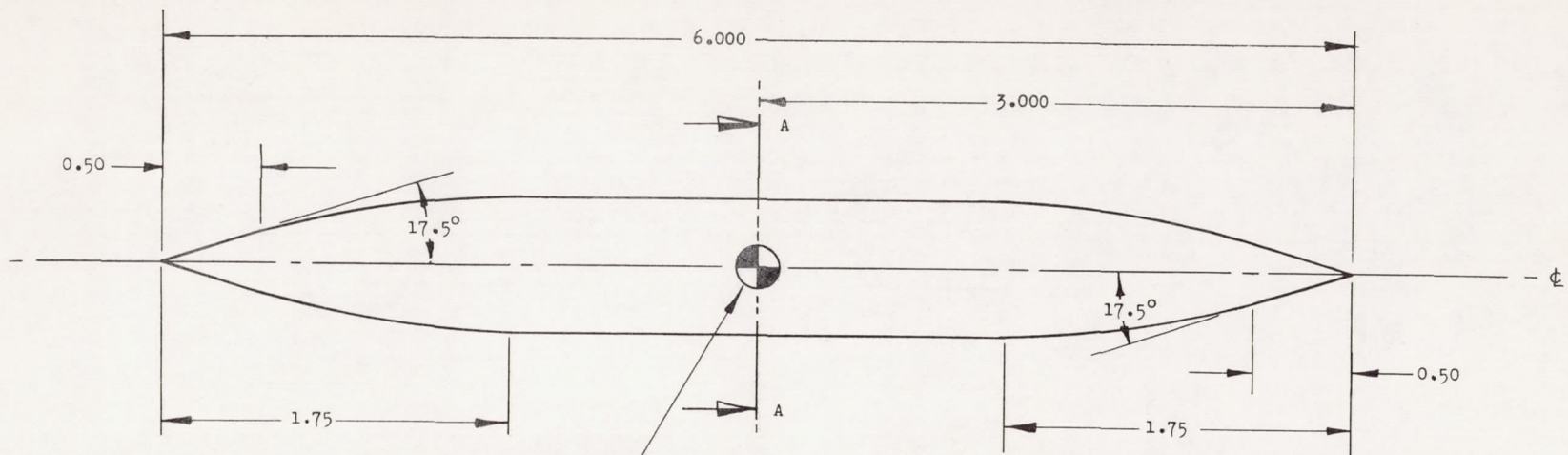




(b) Model 3 with store on.

Figure 1.- Concluded.

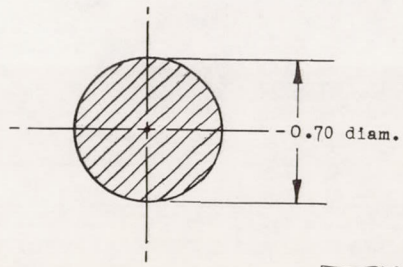




External store c.g.

External Store Ordinates

Station	Radius
0	0
.5	.0157
.750	.236
.815	.256
.891	.275
.993	.294
1.350	.337
1.456	.312
1.750	.350
3.000	.350



Section A-A (Typical)



Figure 2.- Details of external store; diameter, 0.700. All dimensions are in inches.

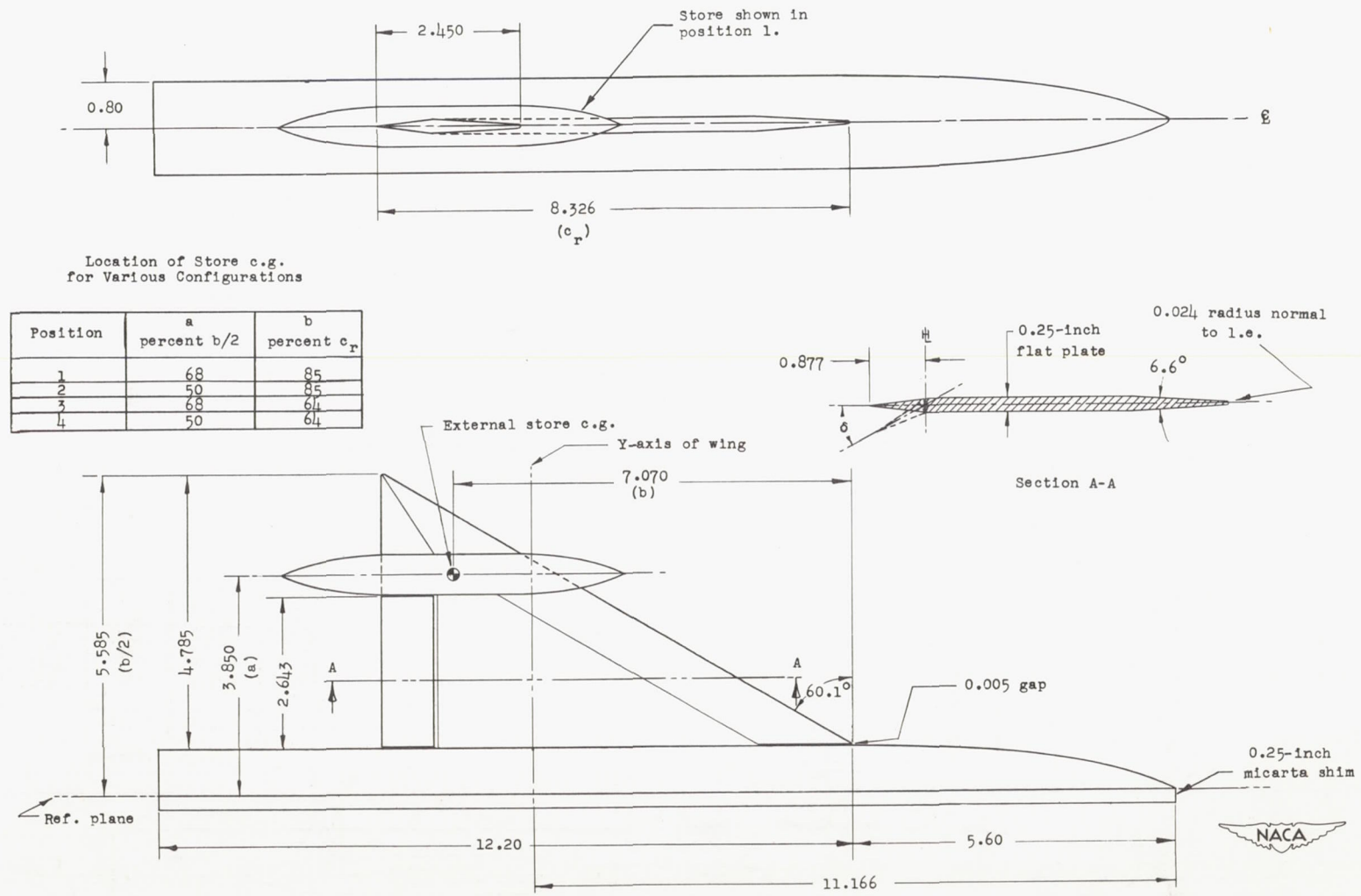


Figure 3.- Details of model 1. 60° delta wing with trailing-edge flap; mean aerodynamic chord, 5.55; span, 11.17. All dimensions are in inches.

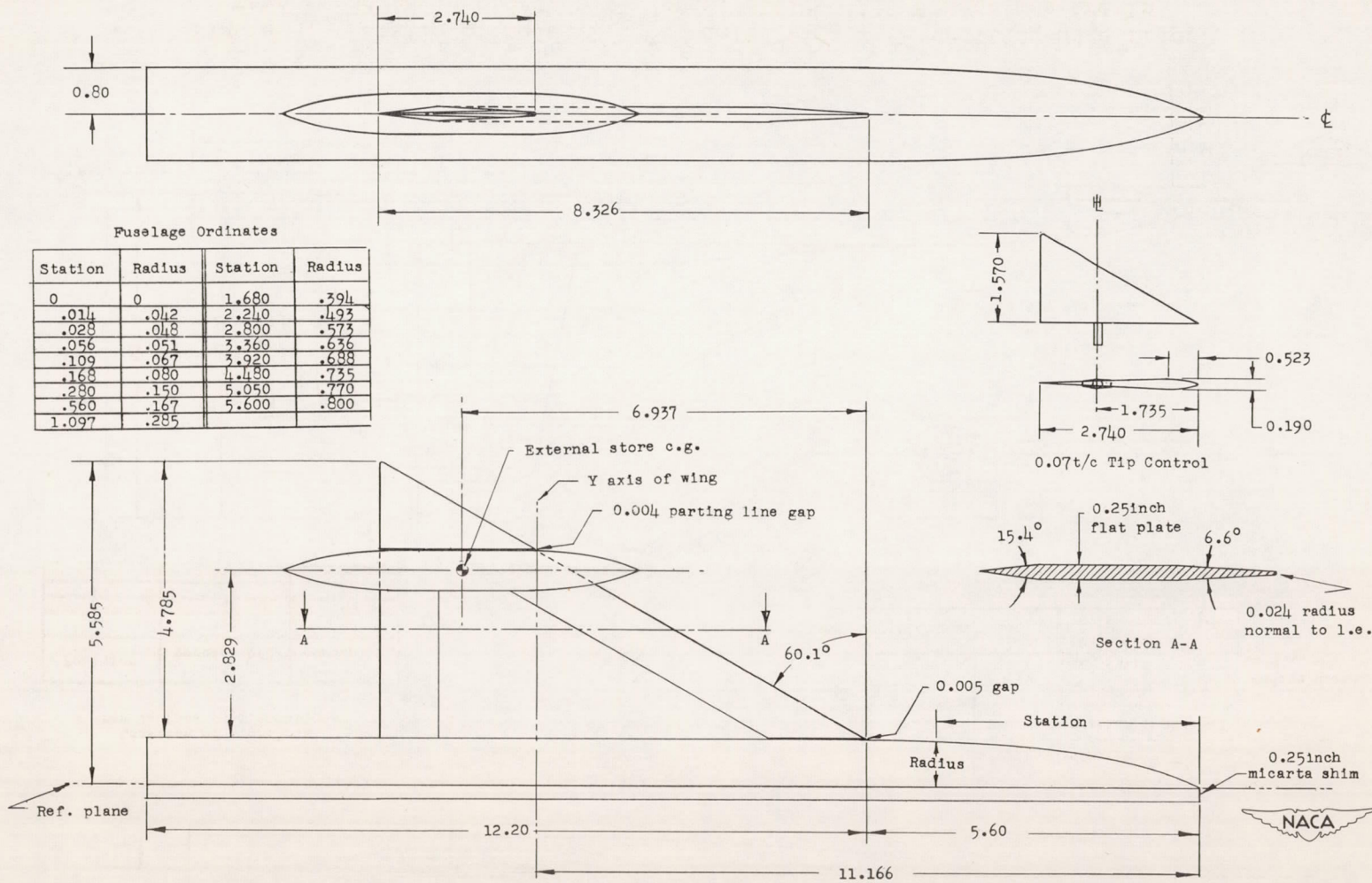


Figure 4.- Details of model 2. 60° delta wing with tip control flap; mean aerodynamic chord, 5.55; span, 11.17. All dimensions are in inches.

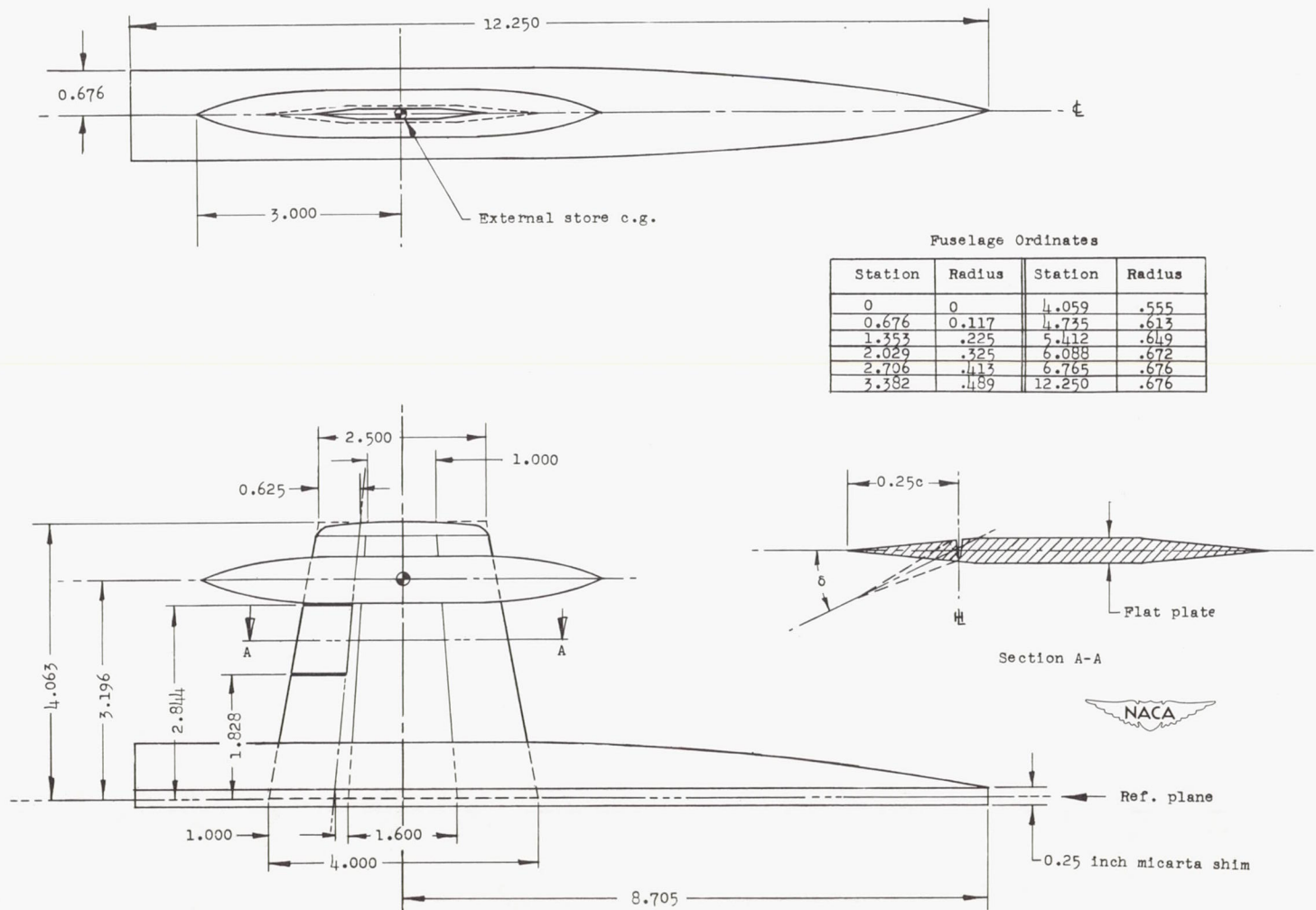


Figure 5.- Details of model 3. 2.5 aspect ratio tapered wing; mean aerodynamic chord 3.131; span, 8.126; taper ratio, 0.625. All dimensions are in inches.

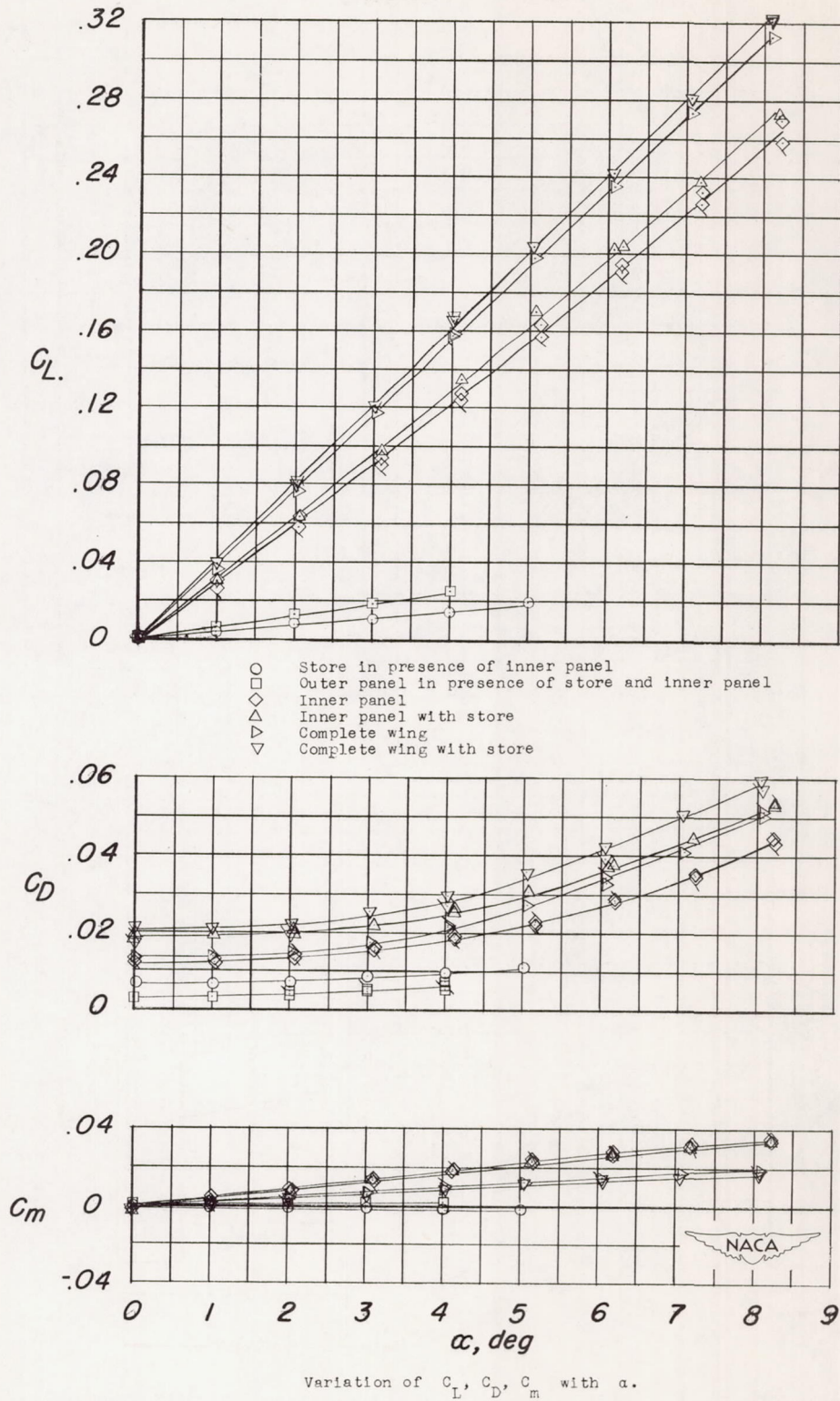
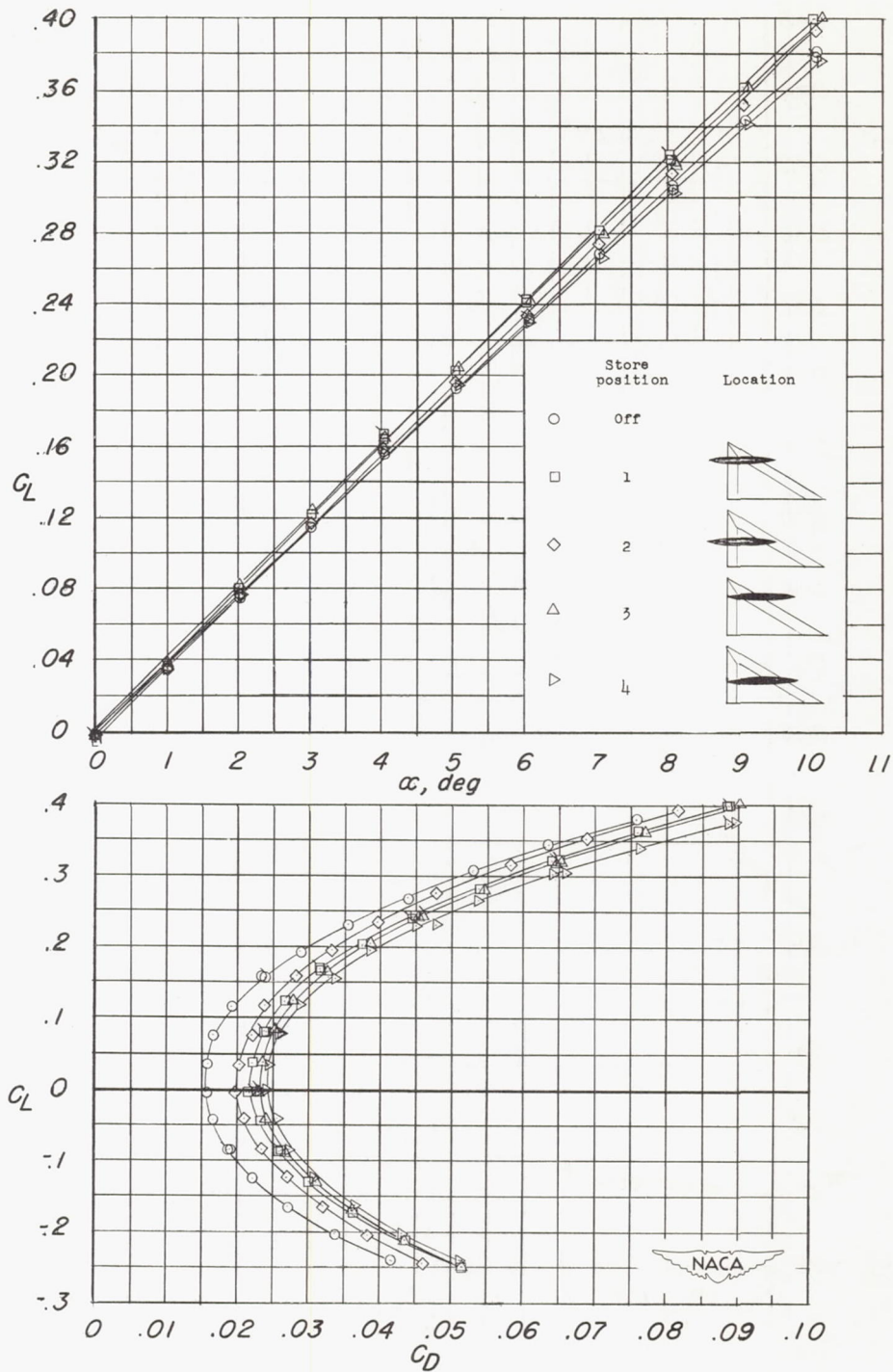
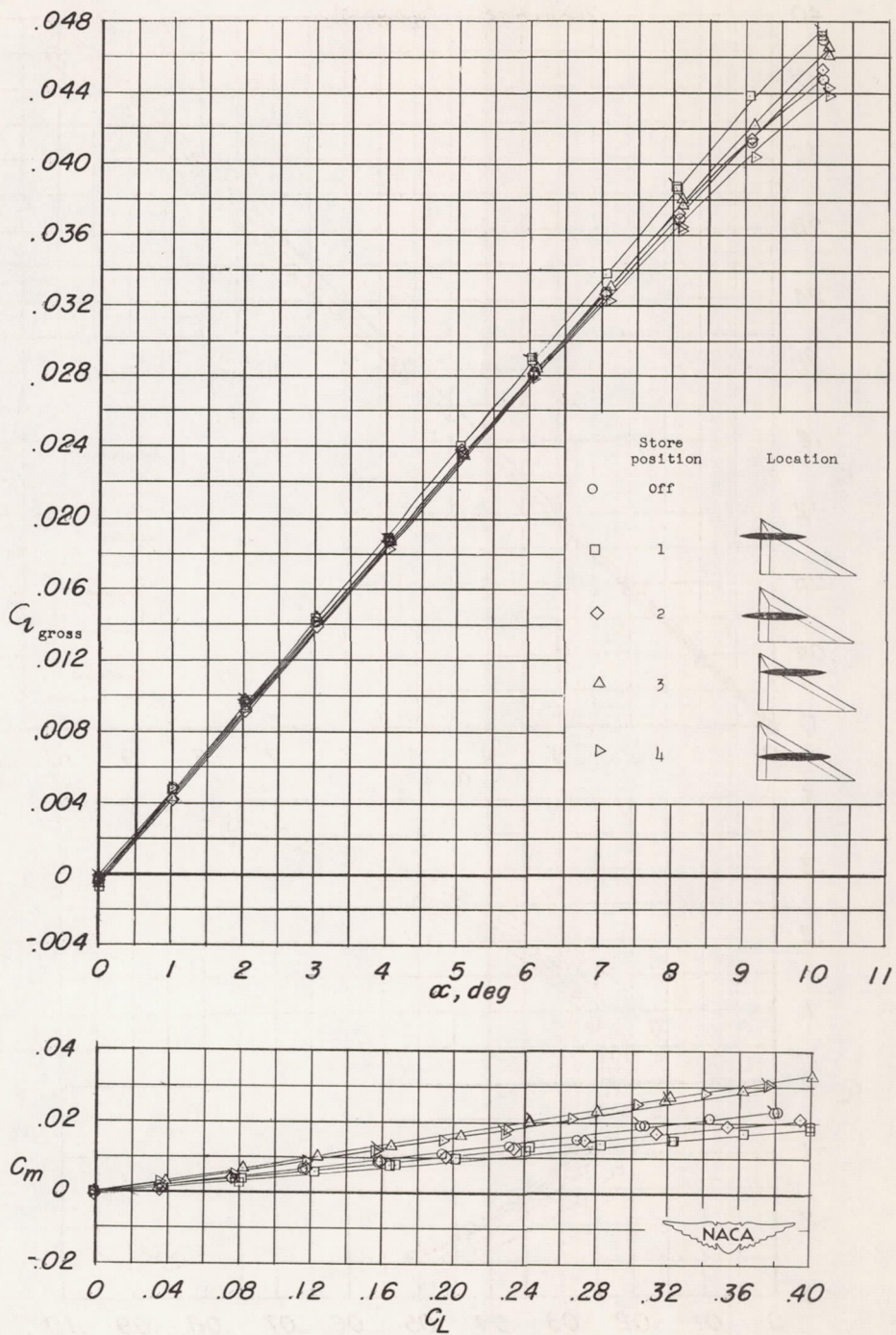


Figure 6.- Breakdown of the aerodynamic loading on the external store, the inner wing panel, and the outer wing panel of a 60° delta wing. $R = 4.0 \times 10^6$. Flagged symbols denote repeat tests.



(a) Variation of C_L with α and C_D .

Figure 7.- Effects of external-store position on the aerodynamic characteristics of a 60° delta wing, control undeflected. $R = 4.0 \times 10^6$. Flagged symbols denote repeat tests.



(b) Variation of $C_{l_{gross}}$ with α and of C_m with C_L .

Figure 7.- Concluded.

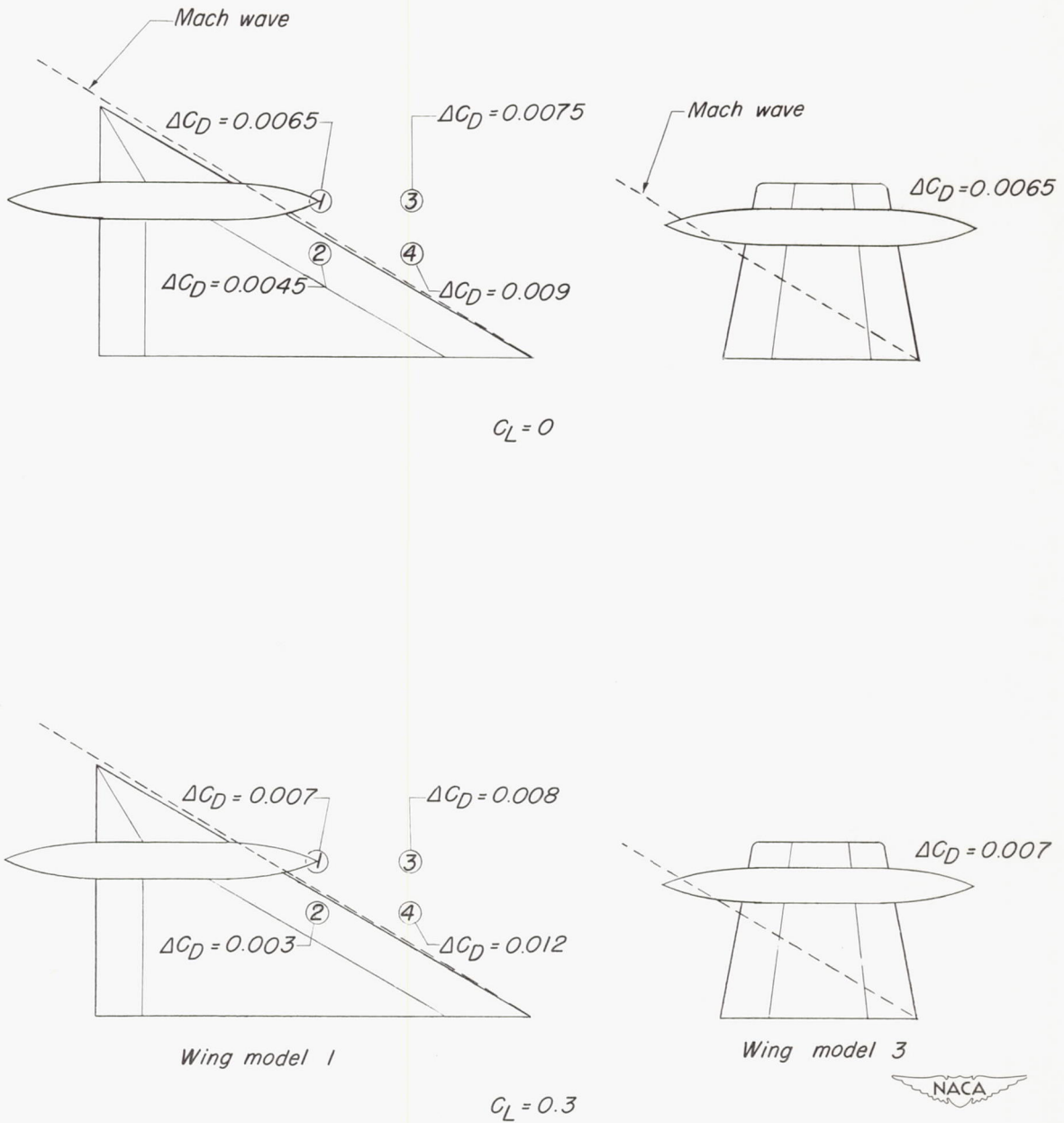
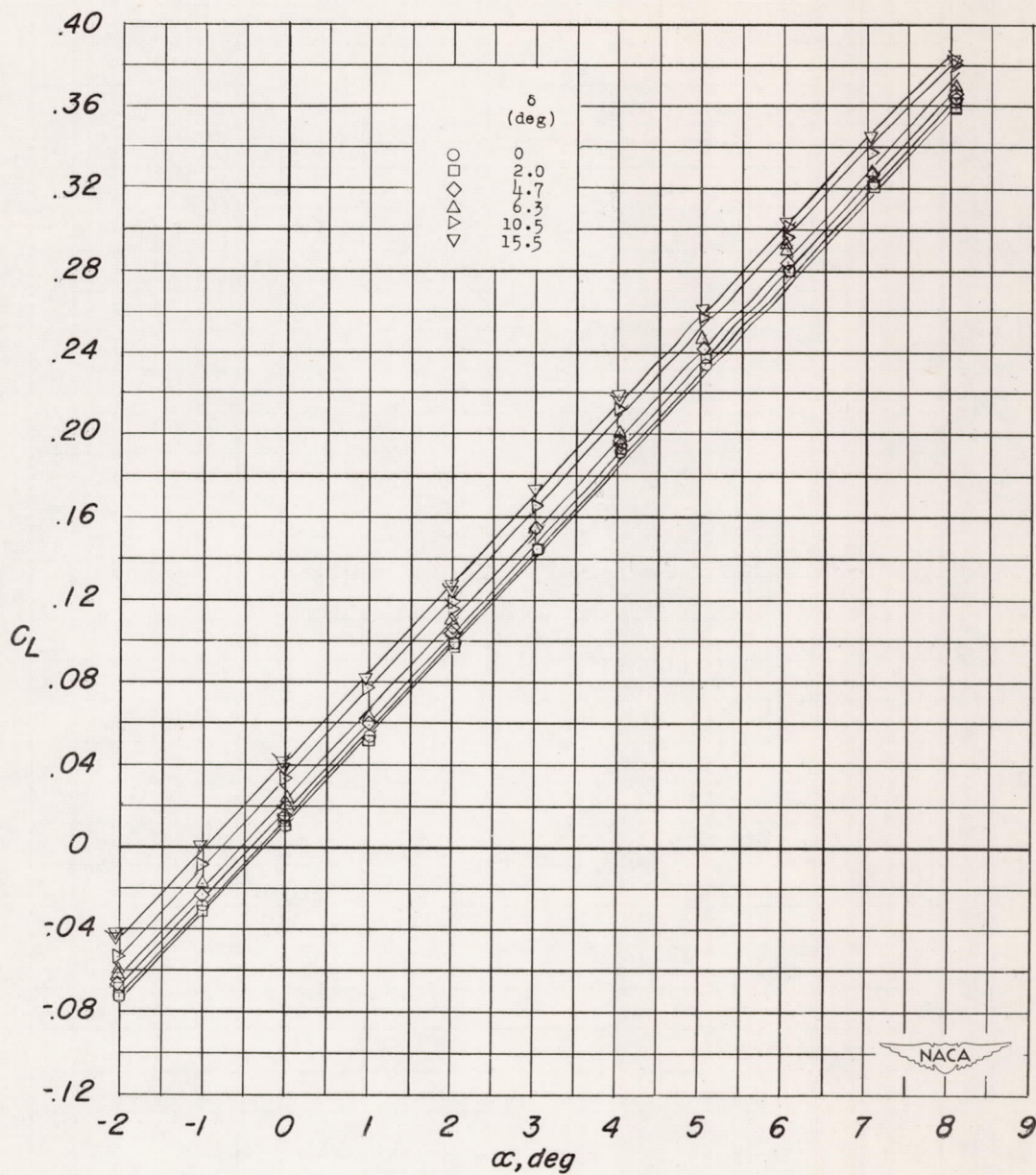
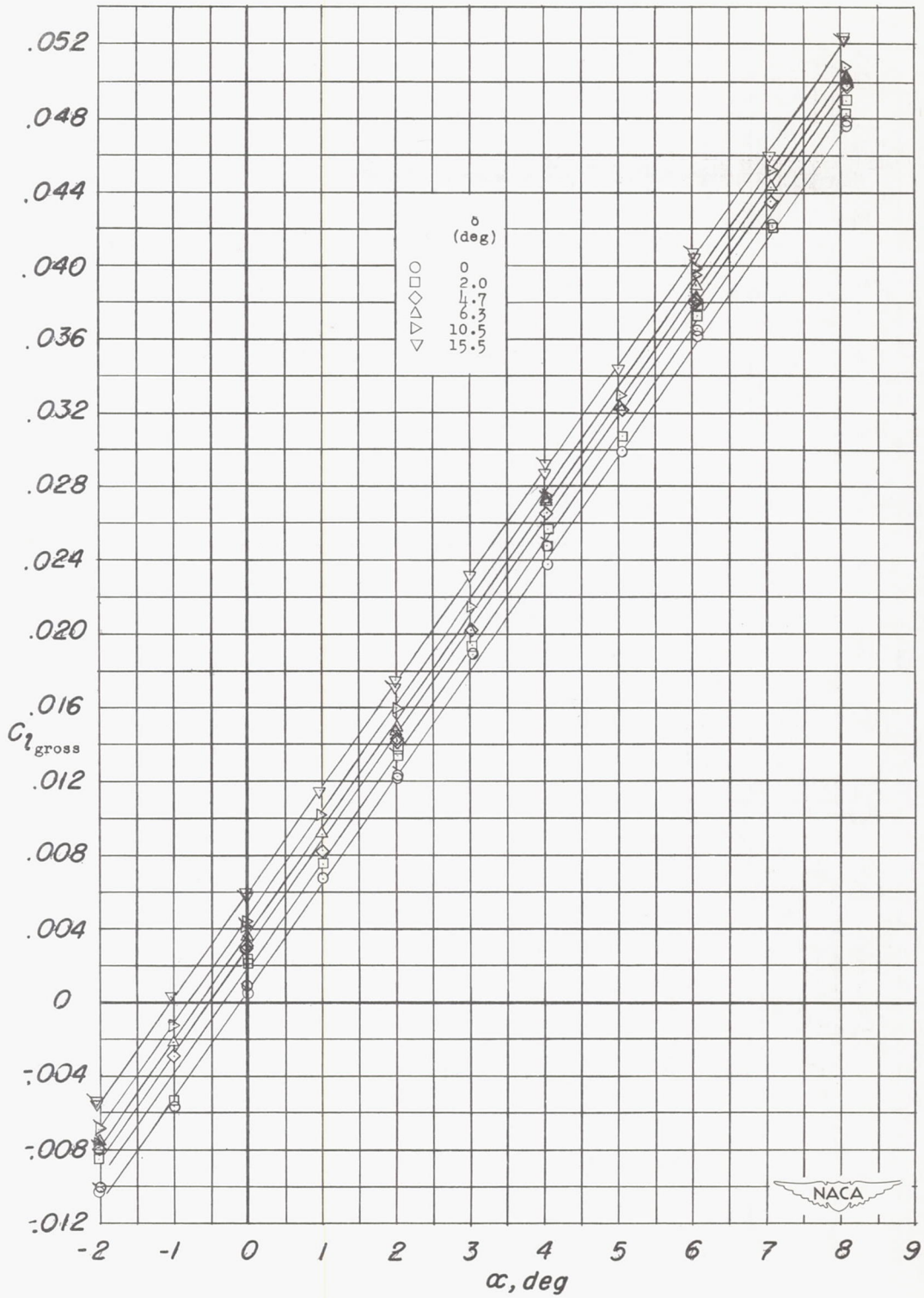


Figure 8.- Increments of drag due to adding the store at various positions on wing models 1 and 3. Numbers on model 1 show location of store nose for each store position. Drag-coefficient increments are based on the wing area of model 1. $M = 1.90$.



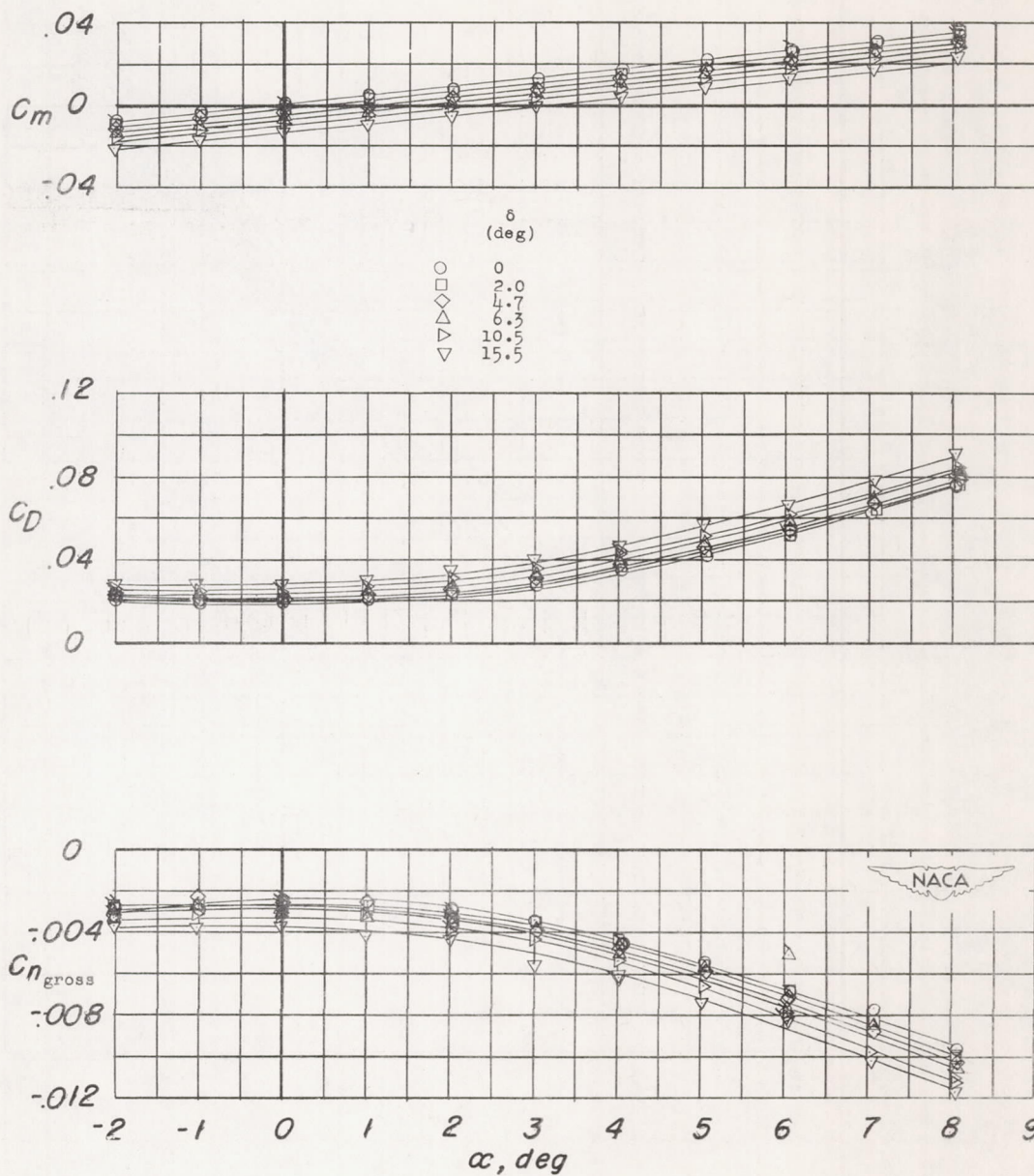
(a) Variation of C_L with α .

Figure 9.- Aerodynamic characteristics of a tapered unswept wing with a 0.25c trailing-edge control. External store off. $R = 2.3 \times 10^6$. Flagged symbols denote repeat tests.



(b) Variation of $C_{l_{gross}}$ with α .

Figure 9.- Continued.



(c) Variation of C_m , C_D , $C_{n_{gross}}$ with α .

Figure 9.- Concluded.

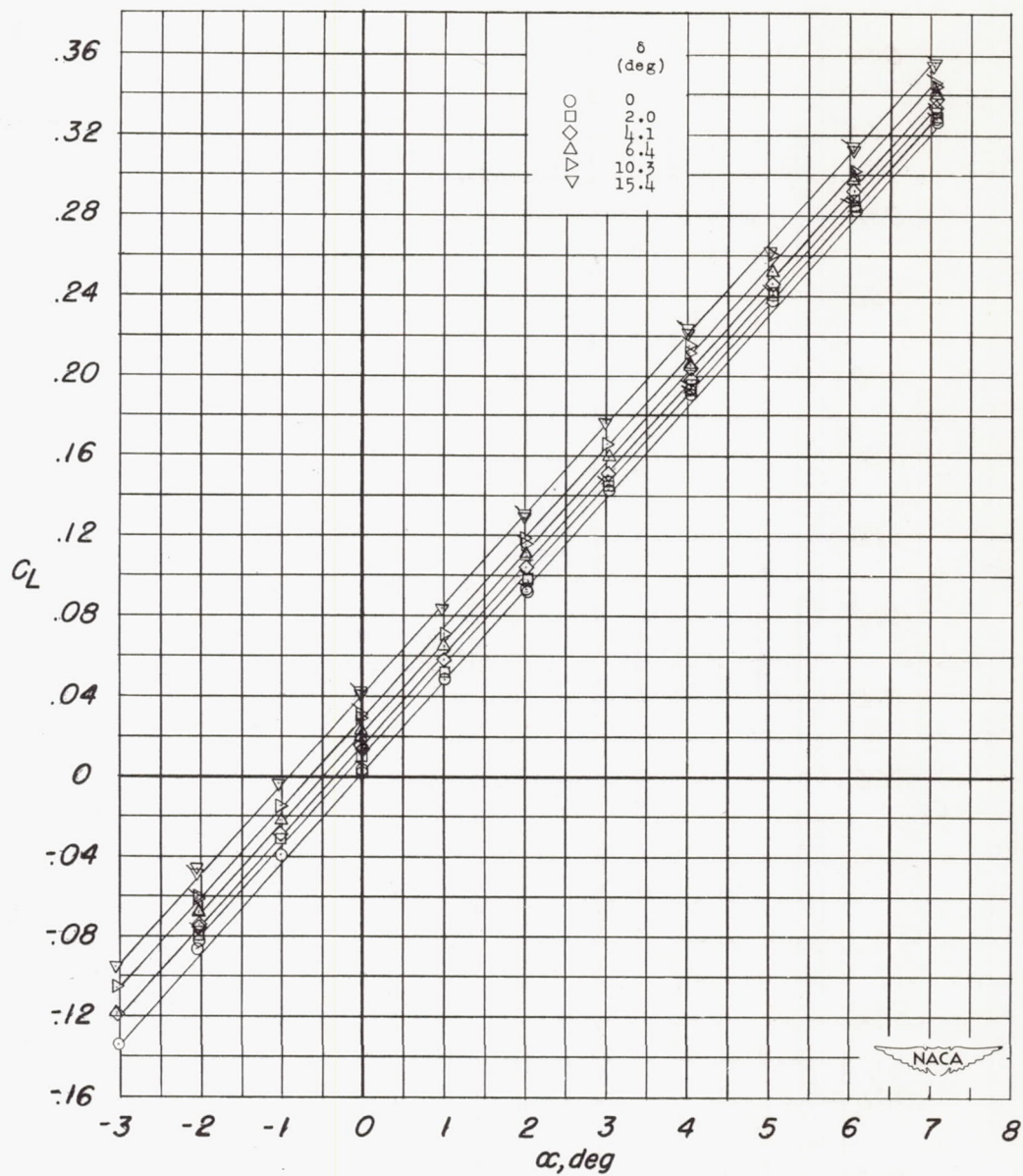
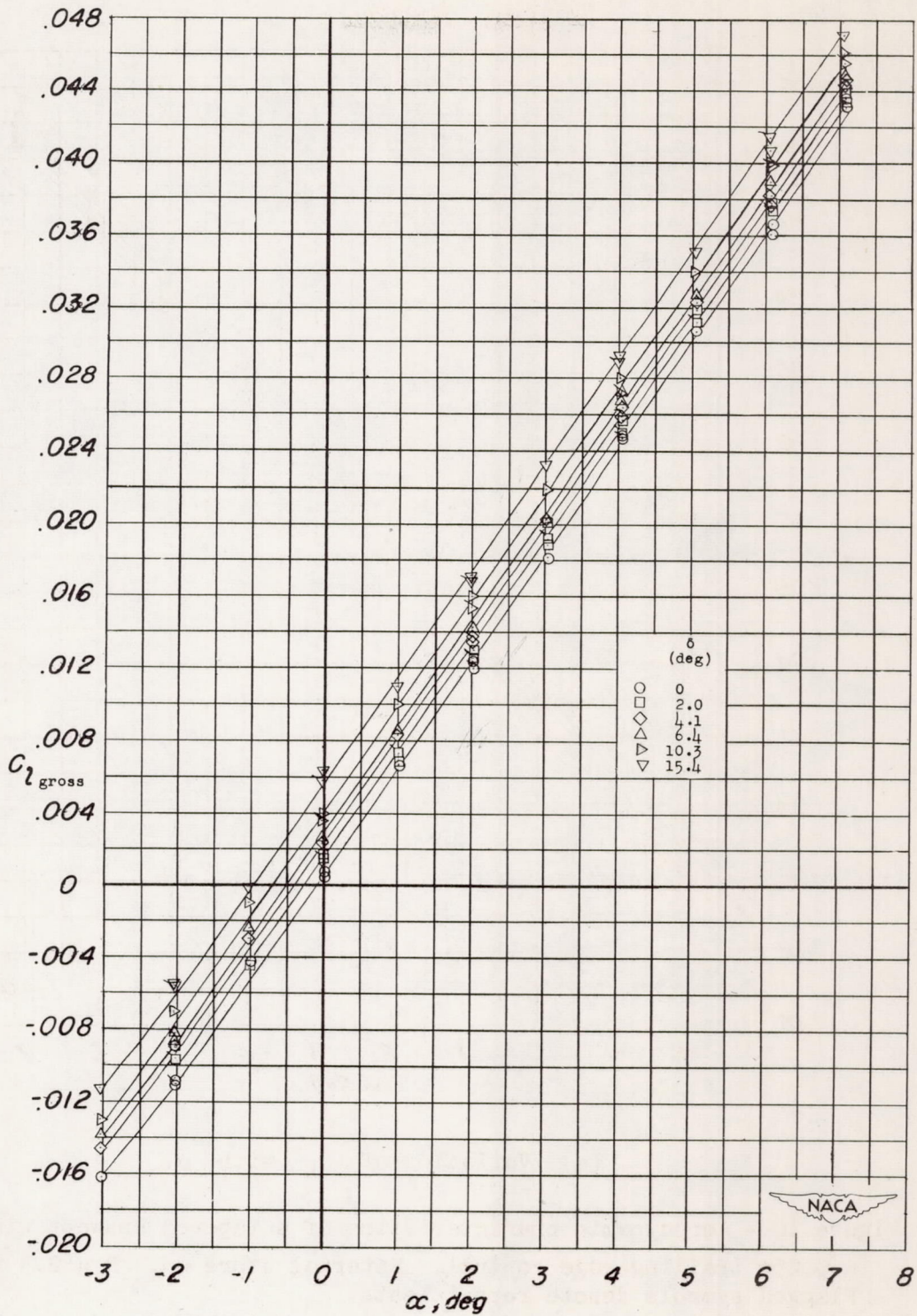
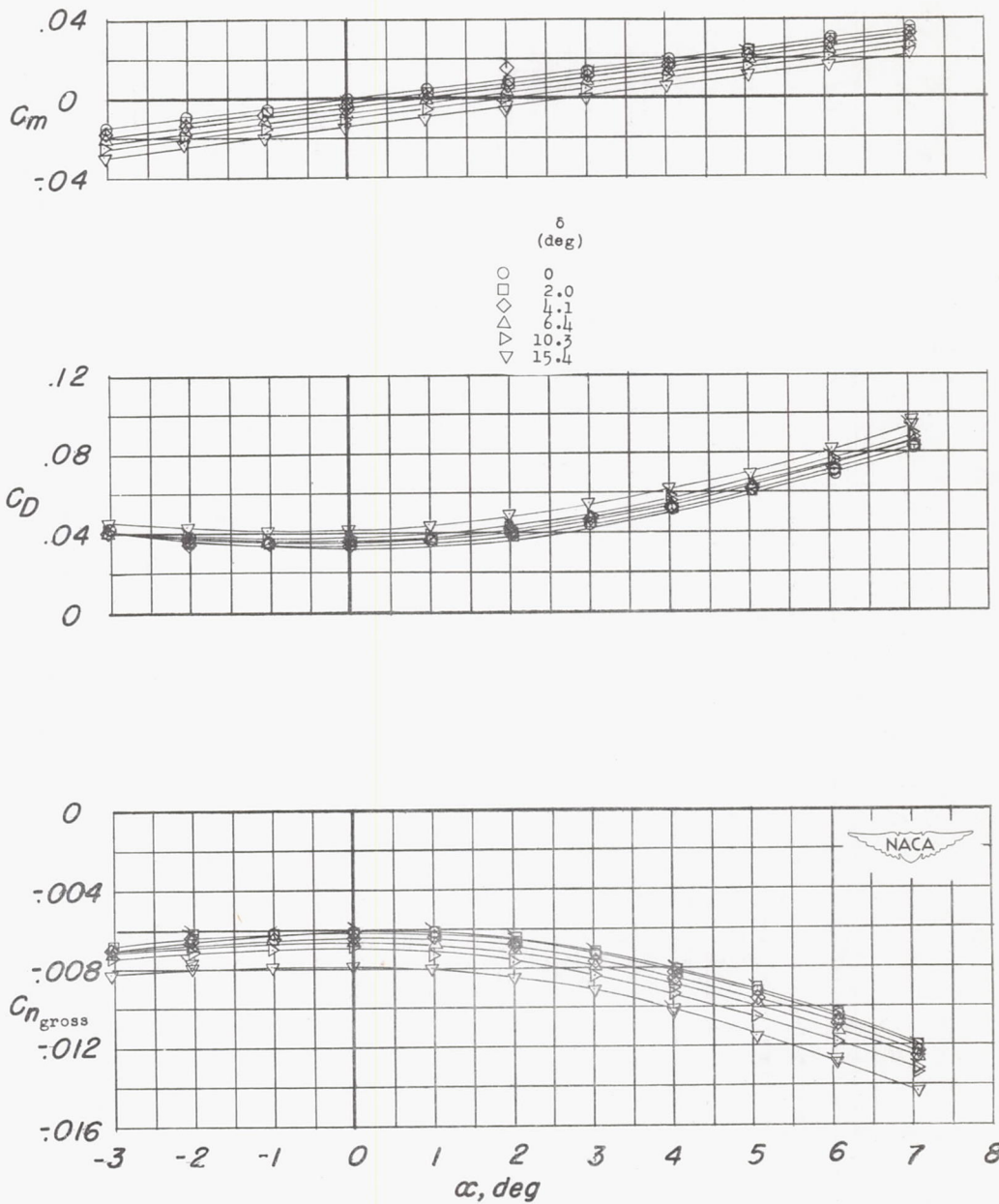
(a) Variation of C_L with α .

Figure 10.- Aerodynamic characteristics of a tapered unswept wing with a 0.25c trailing-edge control. External store on. $R = 2.3 \times 10^6$. Flagged symbols denote repeat tests.



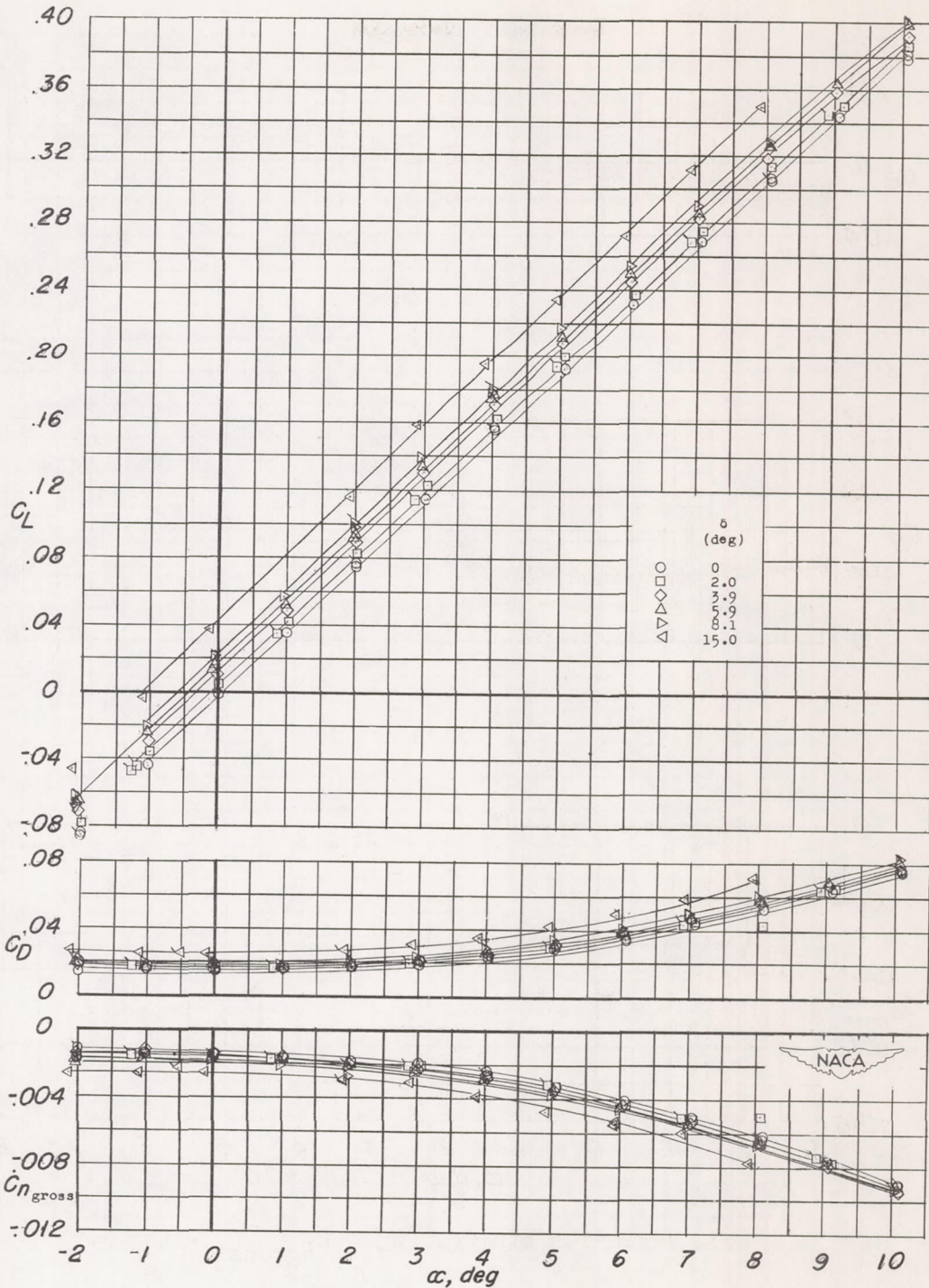
(b) Variation of $C_{l_{gross}}$ with α .

Figure 10.- Continued.



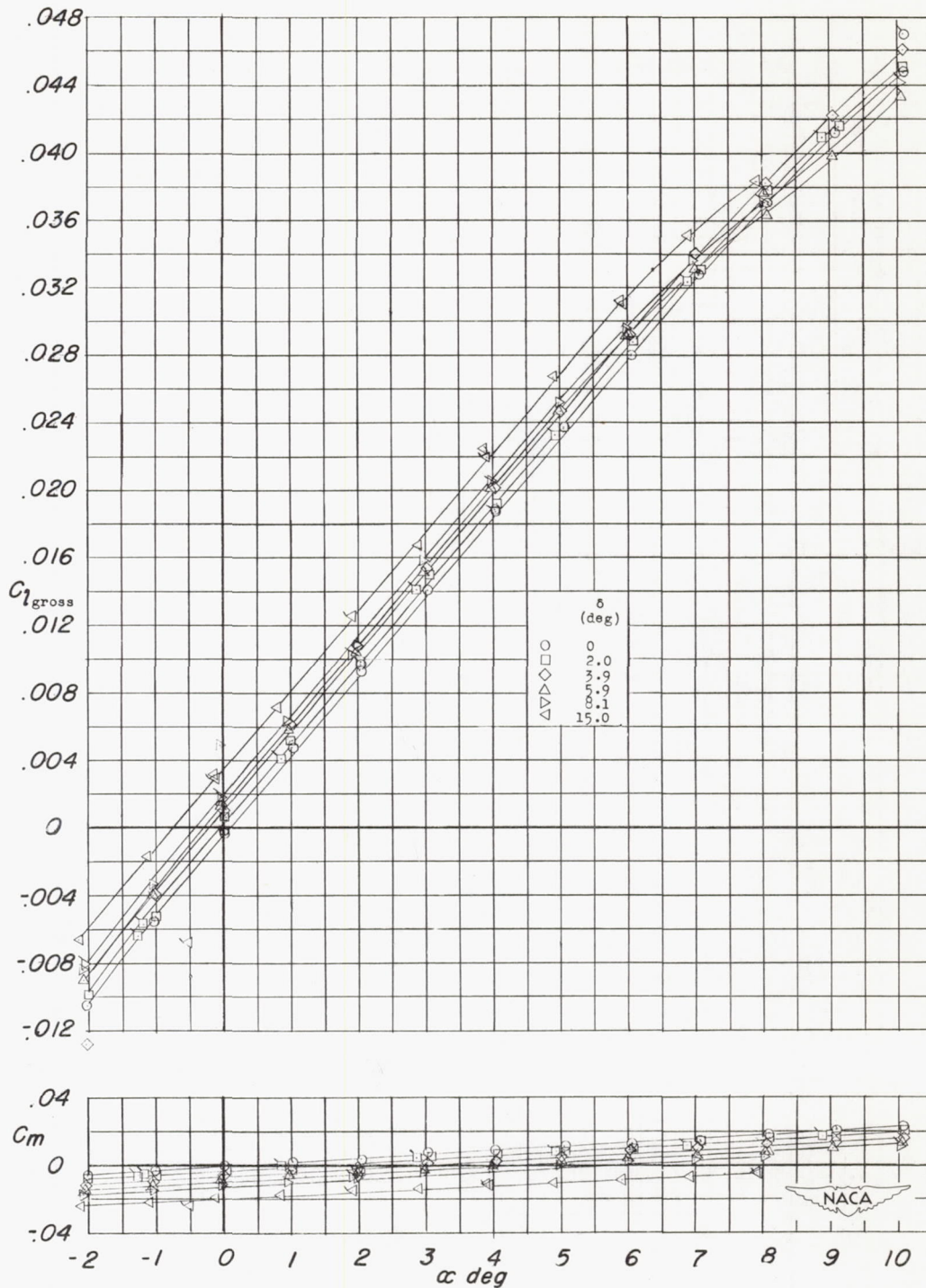
(c) Variation of C_m , C_D , $C_{n_{gross}}$ with α .

Figure 10.- Concluded.



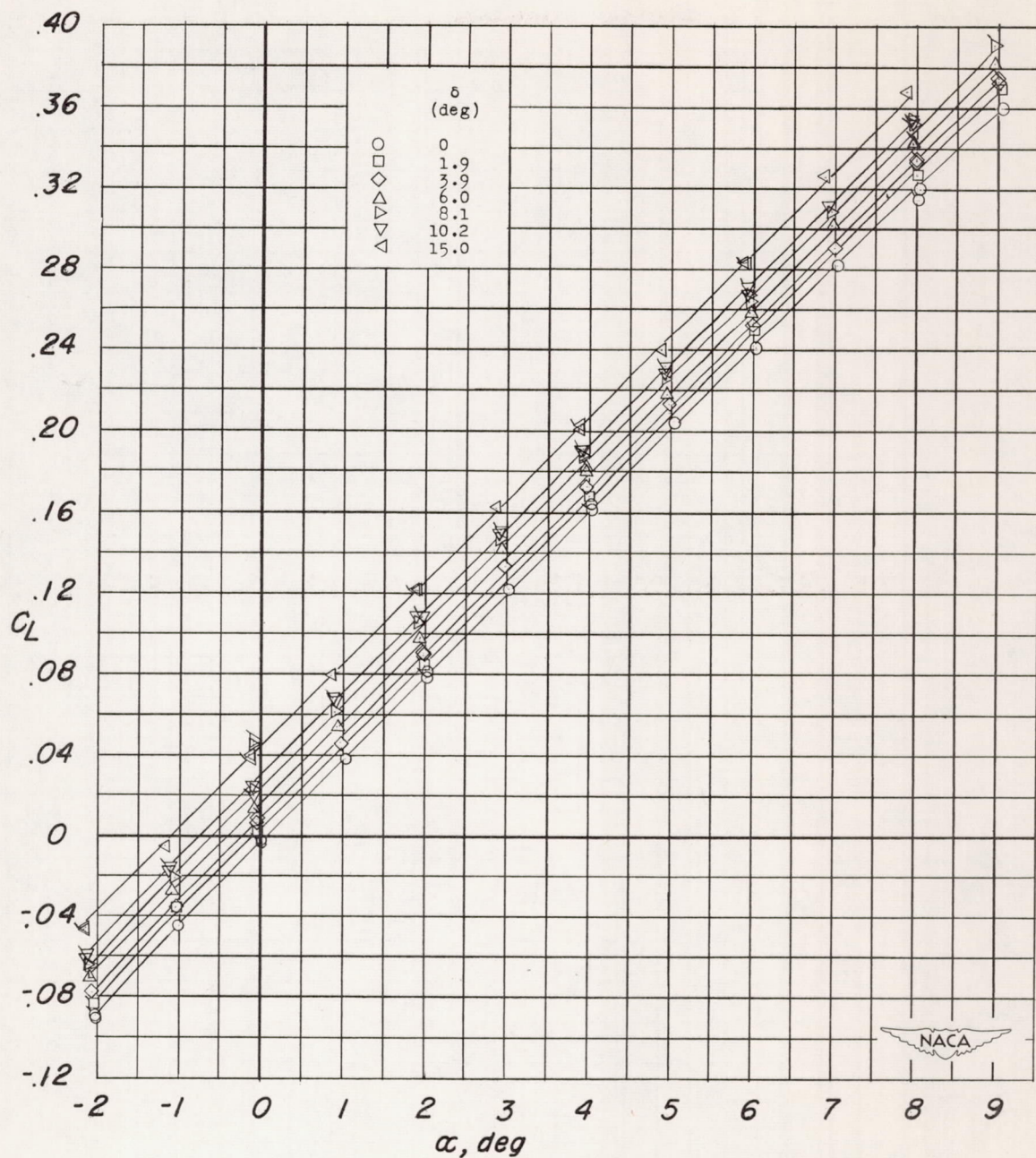
(a) Variation of C_L , C_D , $C_{n_{gross}}$ with α .

Figure 11.- Aerodynamic characteristics of a 60° delta wing with a constant-chord, trailing-edge control. External store off. $R = 4.0 \times 10^6$. Flagged symbols denote repeat tests.



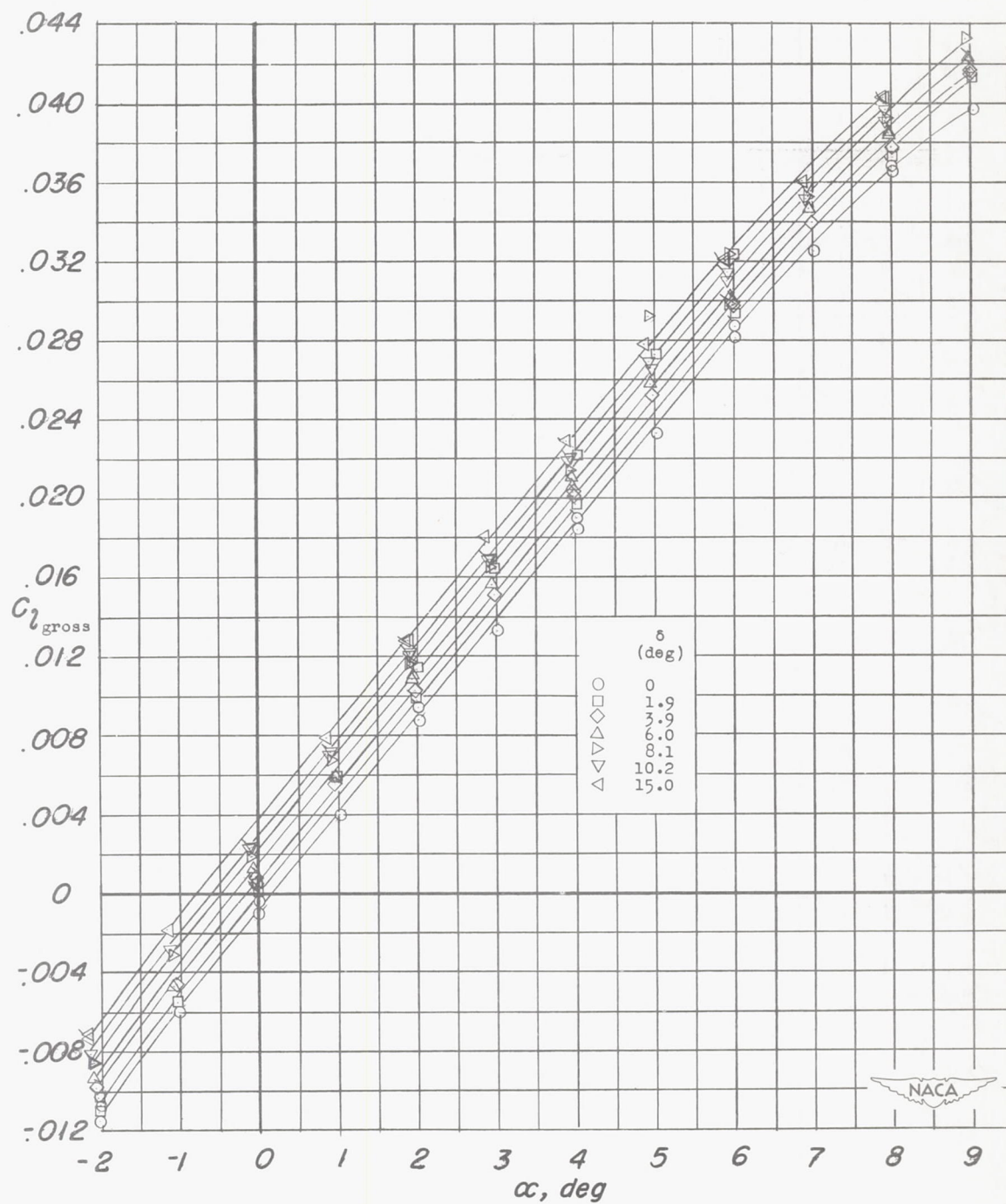
(b) Variation of $C_{l_{gross}}$, C_m with α .

Figure 11.- Concluded.



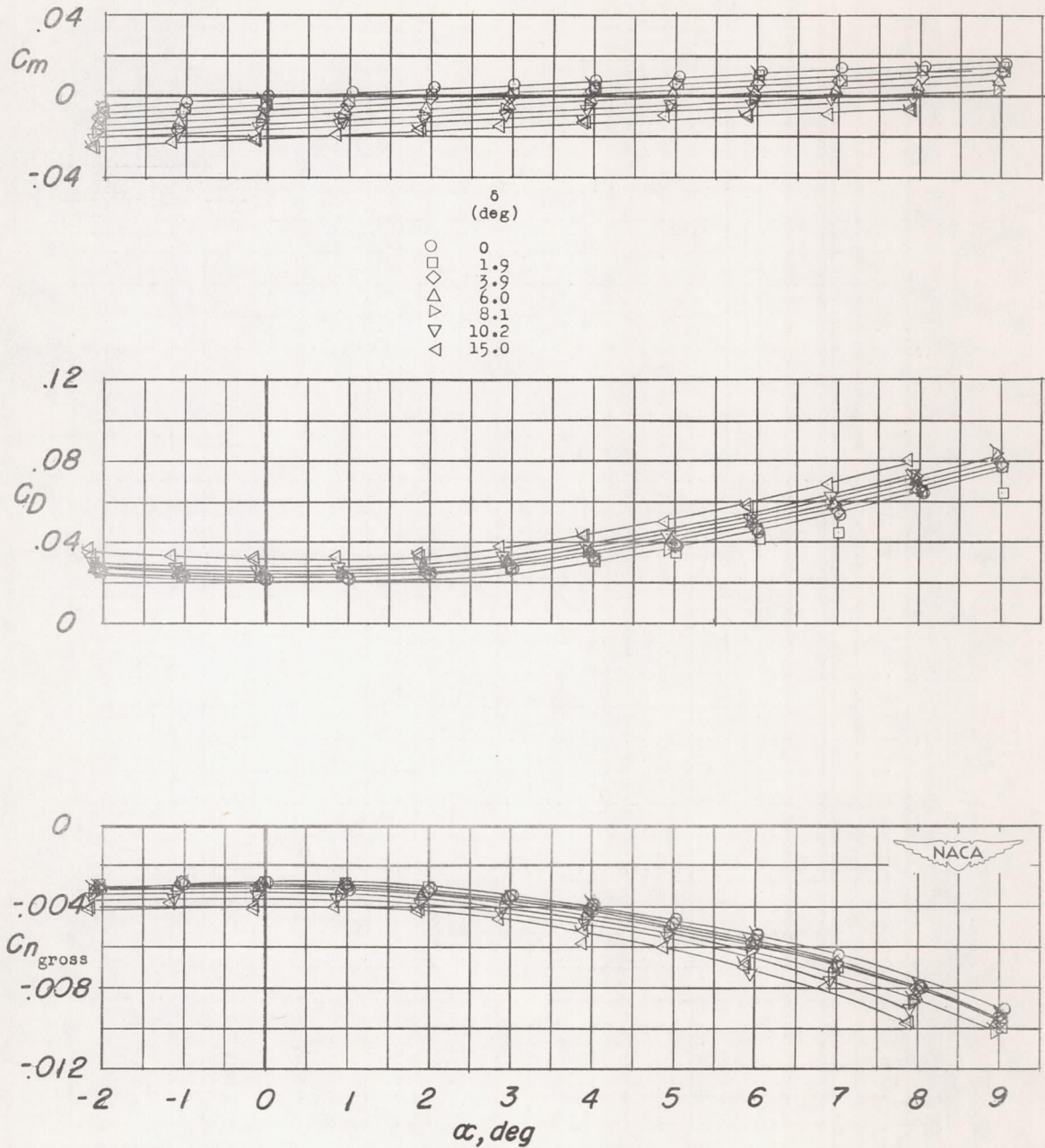
(a) Variation of C_L with α .

Figure 12.- Aerodynamic characteristics of a 60° delta wing with a constant-chord trailing-edge control. External store on. $R = 4.0 \times 10^6$. Flagged symbols denote repeat tests.



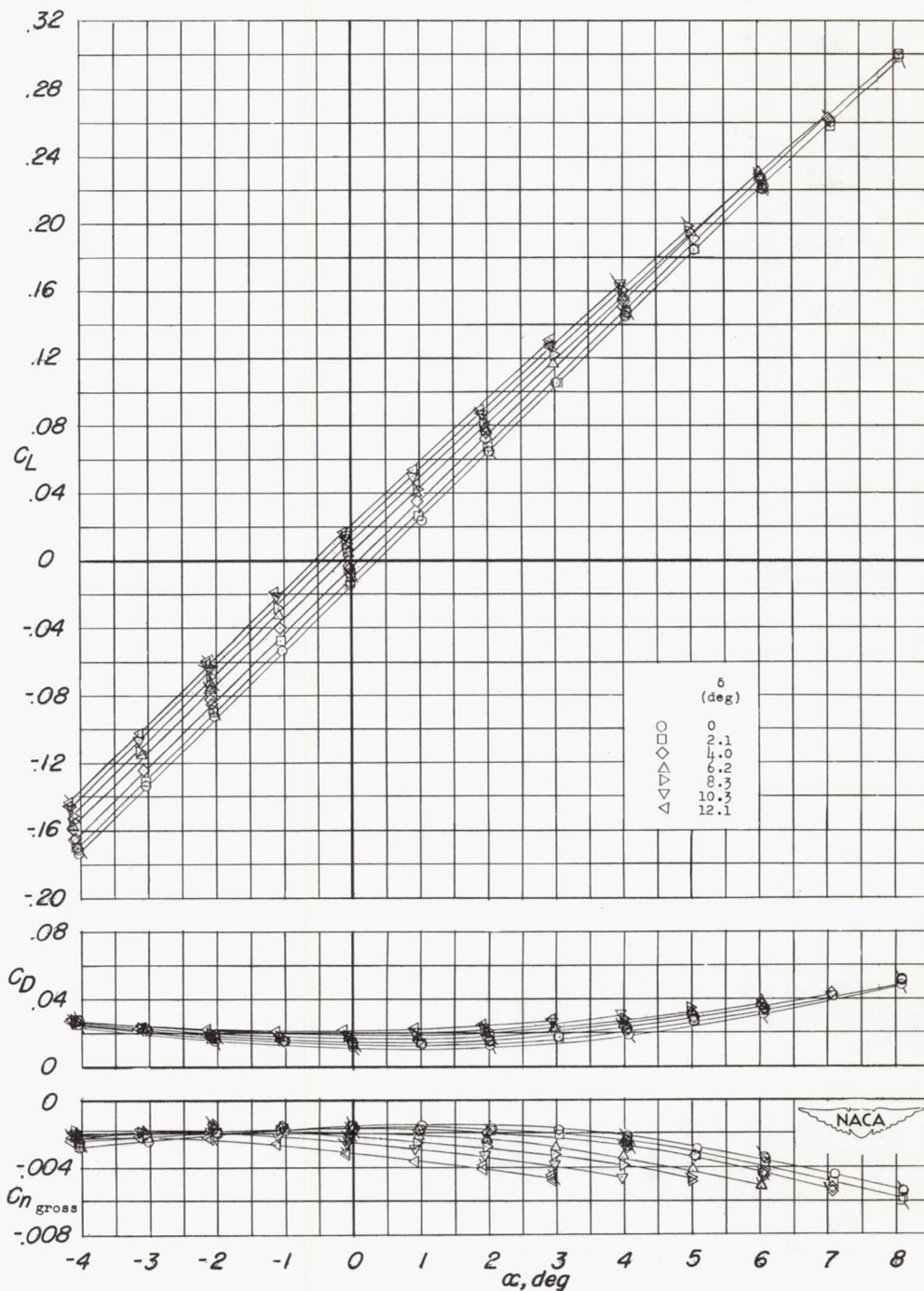
(b) Variation of $C_{l_{gross}}$ with α .

Figure 12.- Continued.



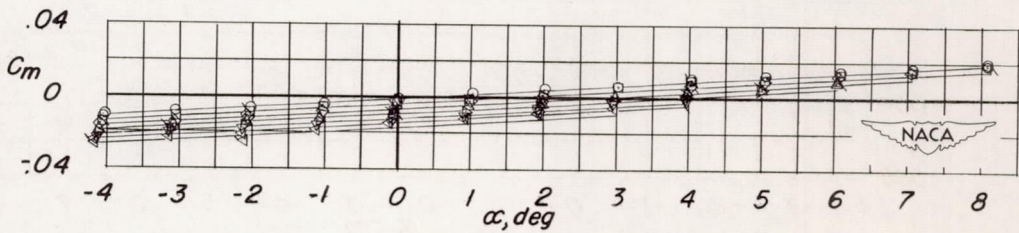
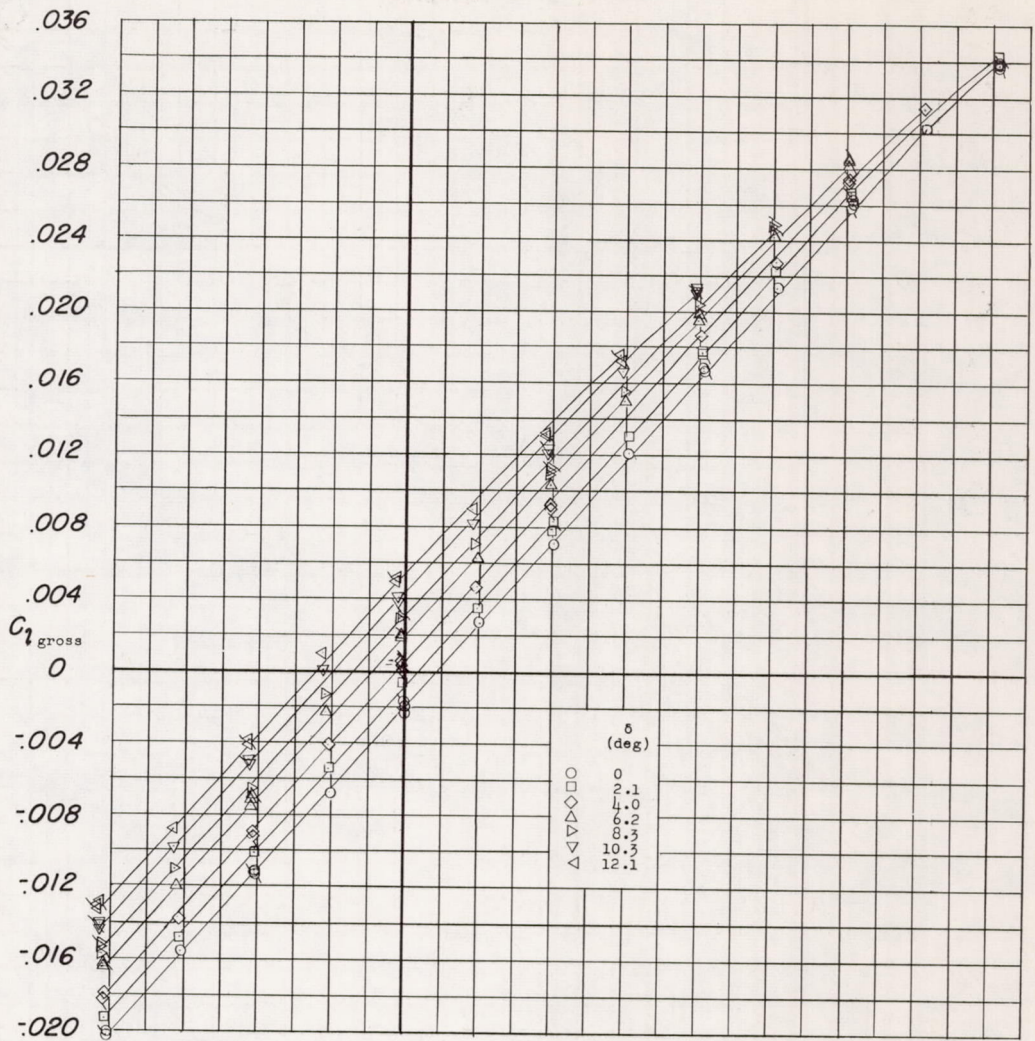
(c) Variation of C_m , C_D , $C_{n_{gross}}$ with α .

Figure 12.- Concluded.



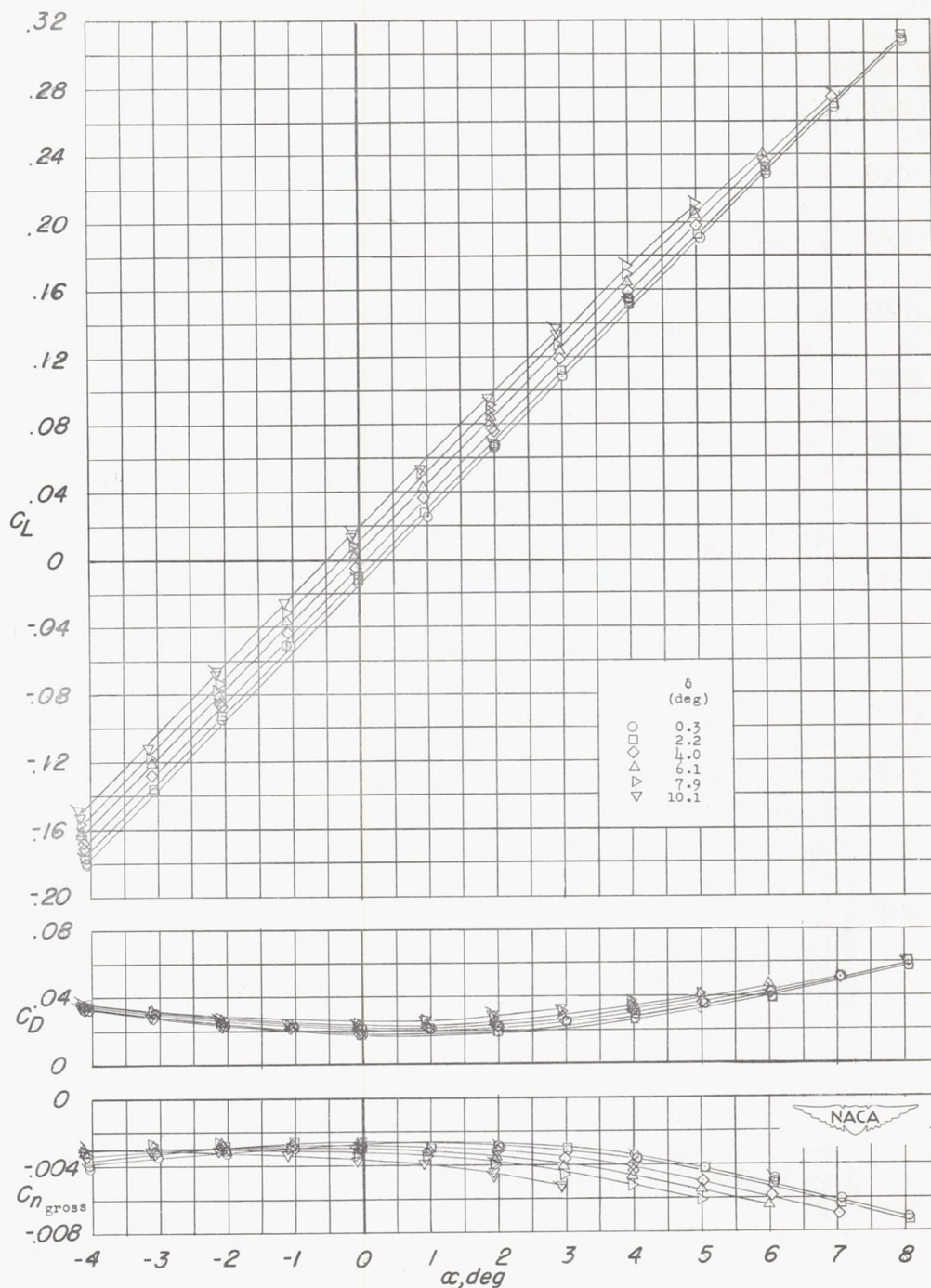
(a) Variation of C_L , C_D , $C_{n_{gross}}$ with α .

Figure 13.- Aerodynamic characteristics of a 60° delta wing with a half-delta tip control. External store off. $R = 4.0 \times 10^6$. Flagged symbols denote repeat tests.



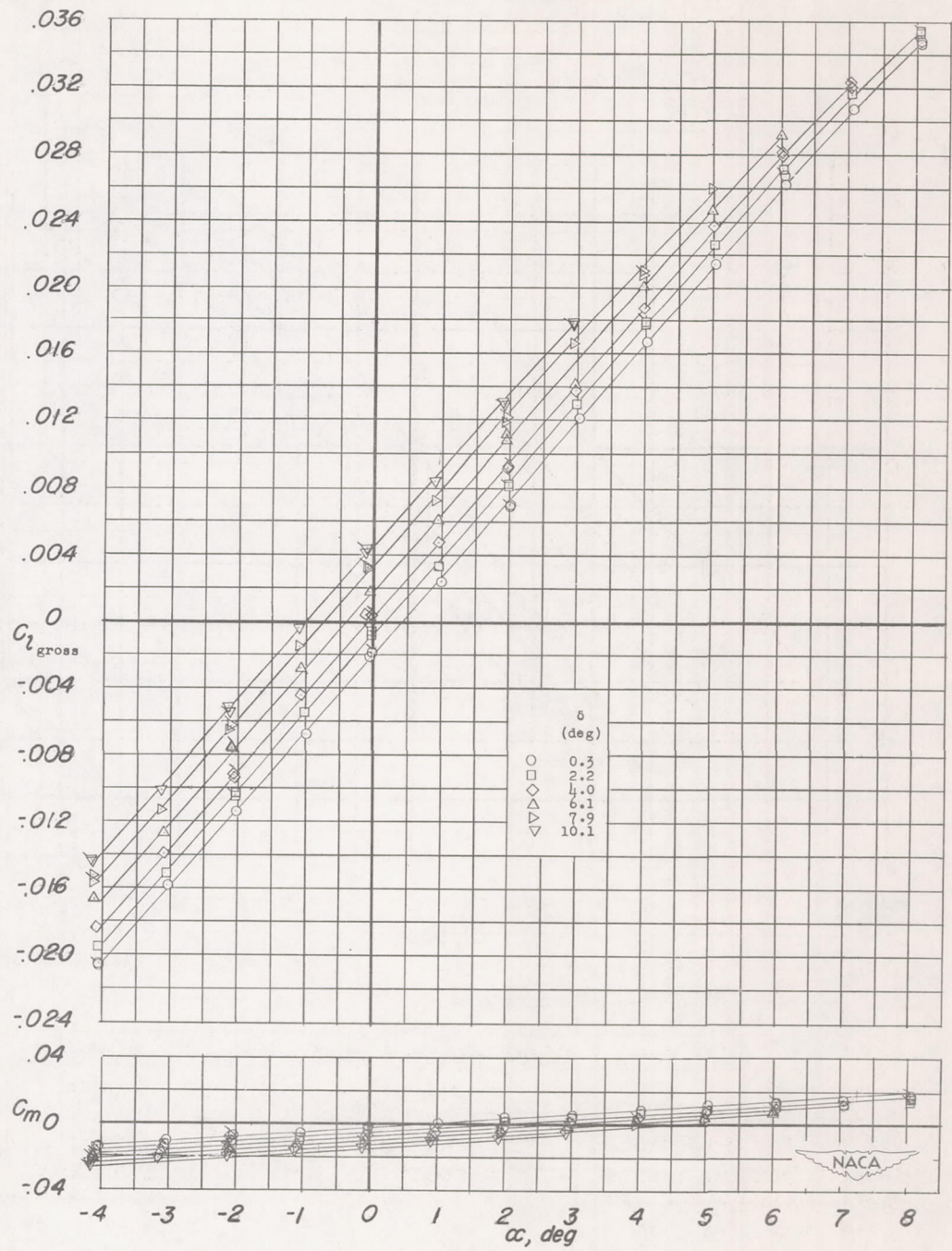
(b) Variation of $C_{l_{gross}}$, C_m with α .

Figure 13.- Concluded.



(a) Variation of C_L , C_D , $C_{n_{gross}}$ with α .

Figure 14.- Aerodynamic characteristics of a 60° delta wing with a half-delta tip control. External store on. $R = 4.0 \times 10^6$. Flagged symbols denote repeat tests.



(b) Variation of $C_{l_{gross}}$, C_m with α .

Figure 14.- Concluded.

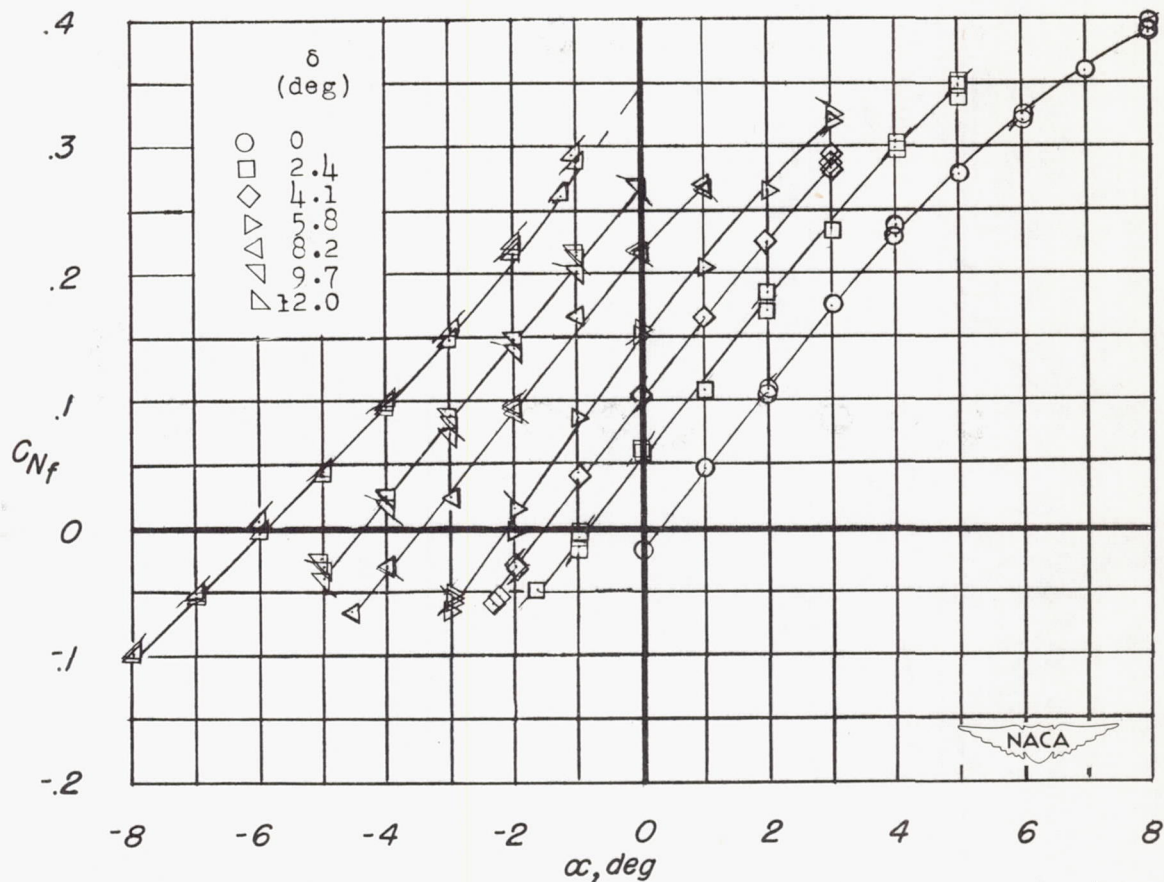
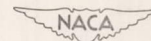
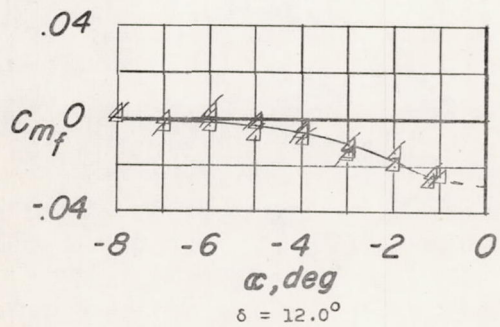
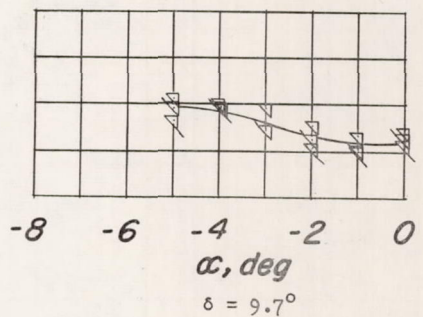
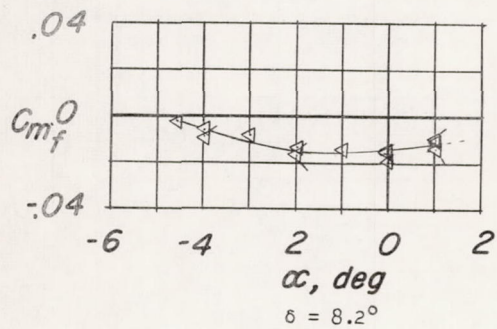
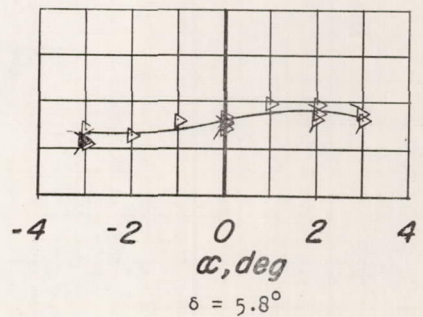
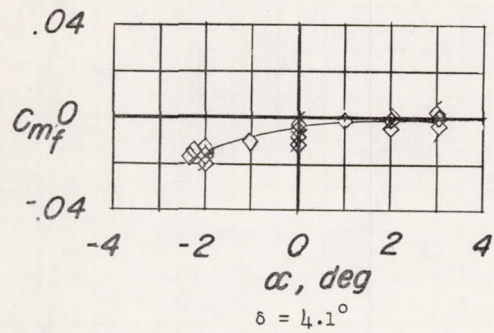
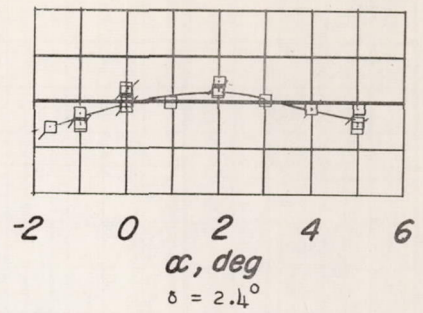
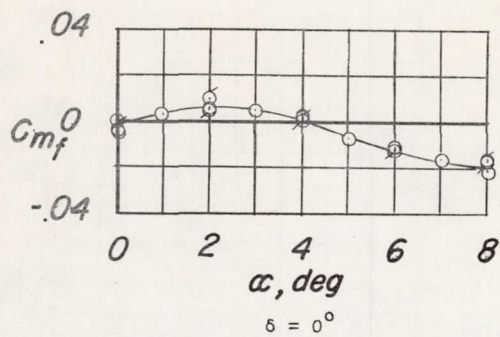
(a) Normal force plotted against α .

Figure 15.- Aerodynamic loading characteristics of a half-delta tip control on a 60° delta wing tested in presence of the inner wing panel. External store off. Data presented with respect to control-surface axes. Flagged symbols denote repeat tests.

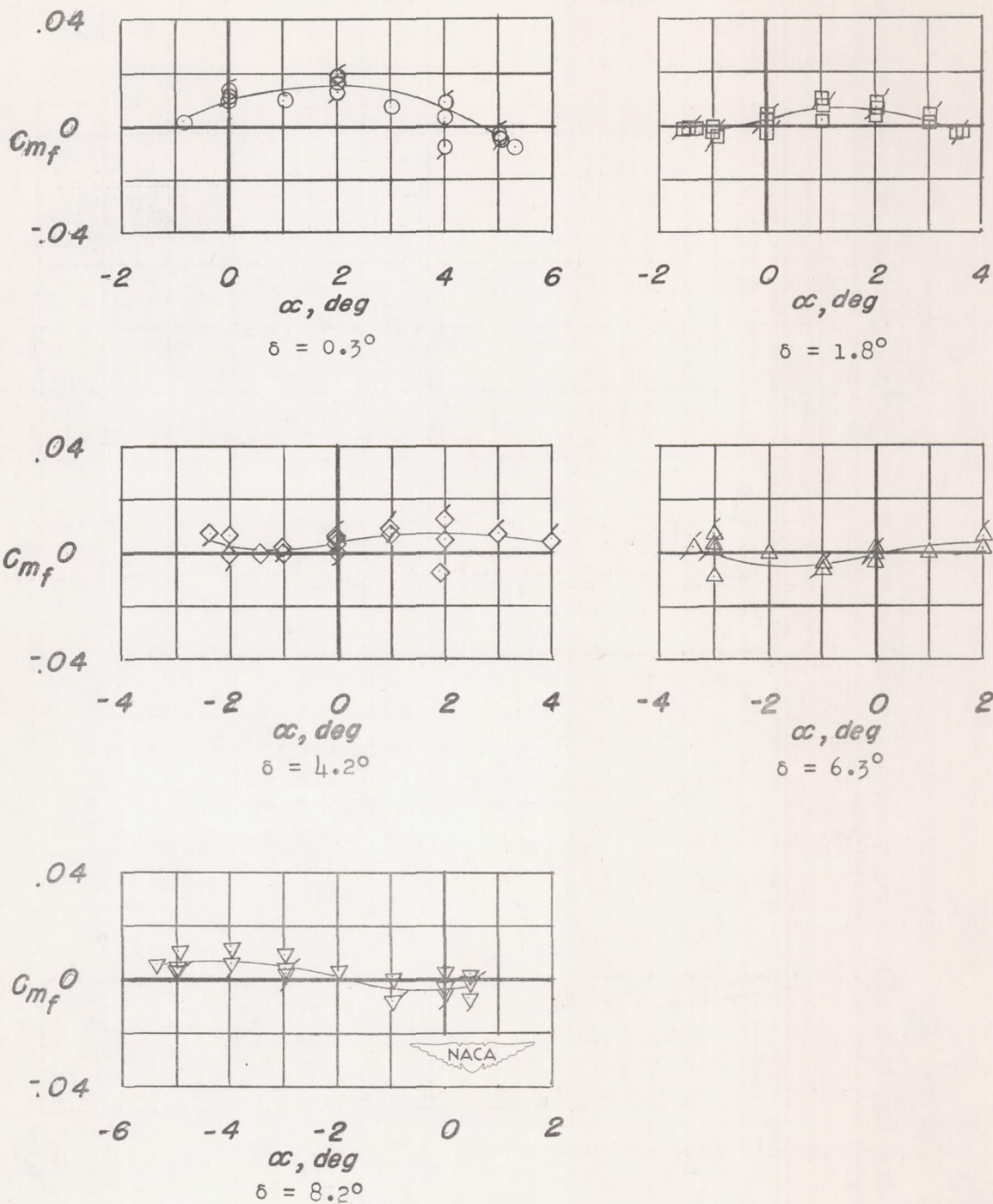


(b) Hinge moment plotted against α .

Figure 15.- Concluded.

(a) Normal force plotted against α .

Figure 16.- Aerodynamic loading characteristics of a half-delta tip control on a 60° delta wing tested in the presence of the inner wing panel. External store on. Data presented with respect to control-surface axes. Flagged symbols denote repeat tests.



(b) Hinge moment plotted against α .

Figure 16.- Concluded.

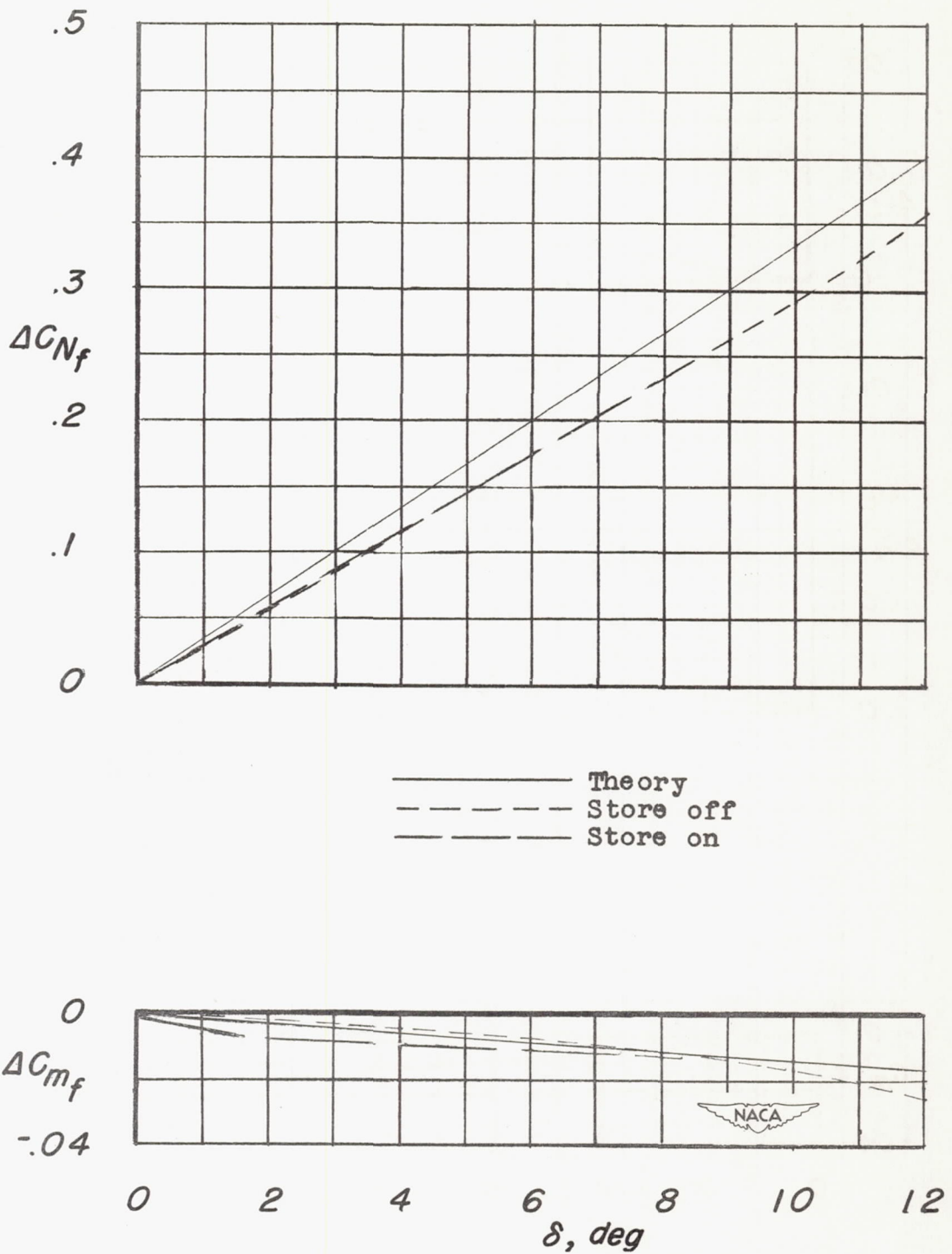


Figure 17.- Variation of the aerodynamic loading characteristics of a half-delta tip control on a 60° delta wing tested in the presence of the inner wing panel. External store off and on. $R = 4.0 \times 10^6$; $M = 1.90$; $\alpha = 0^\circ$.

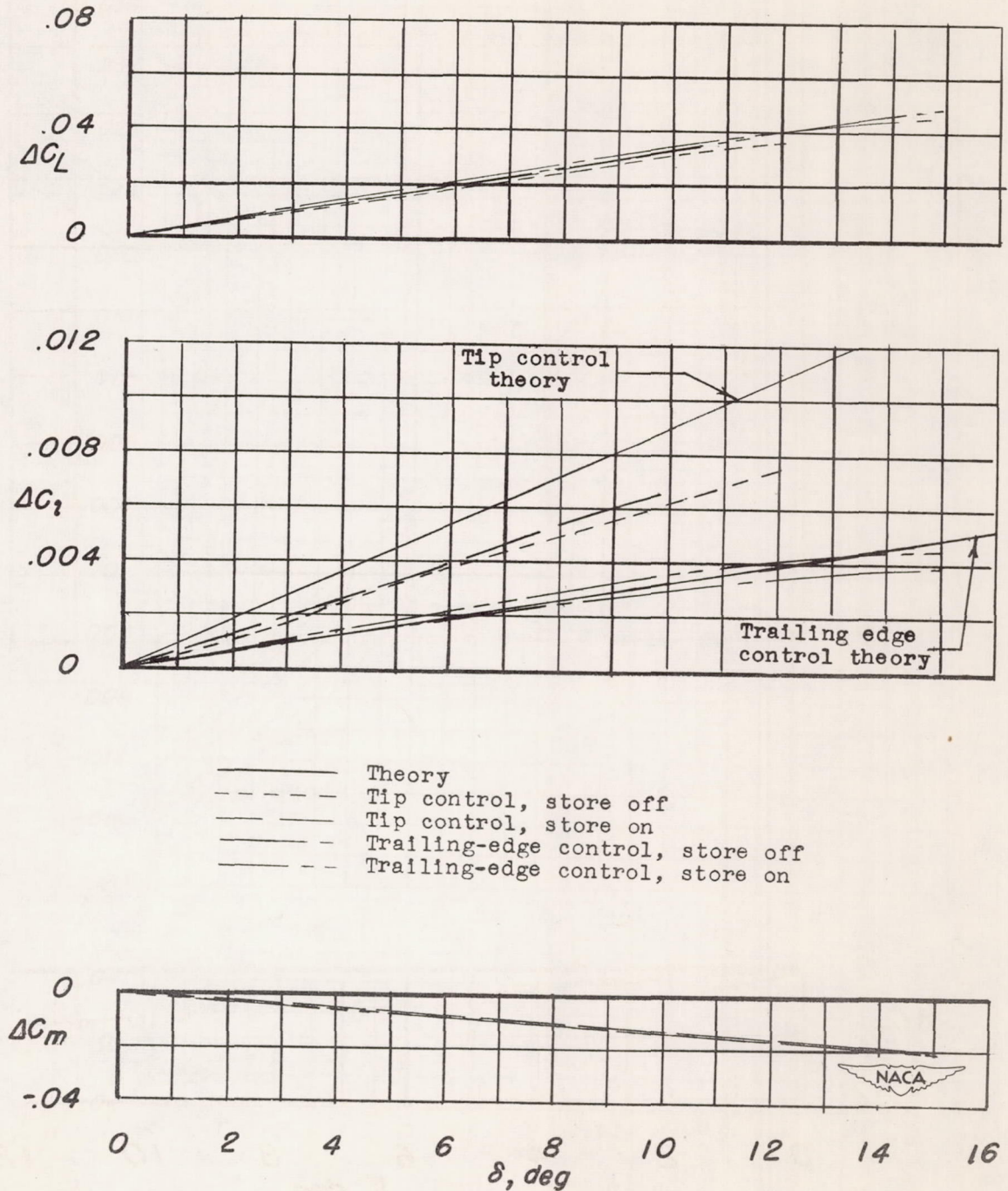


Figure 18.- Variation of the aerodynamic characteristics with control deflection of a 60° delta wing with a full-chord tip control and a trailing-edge control. External store off and on. $R = 4.0 \times 10^6$; $M = 1.90$; $\alpha = 0^\circ$.

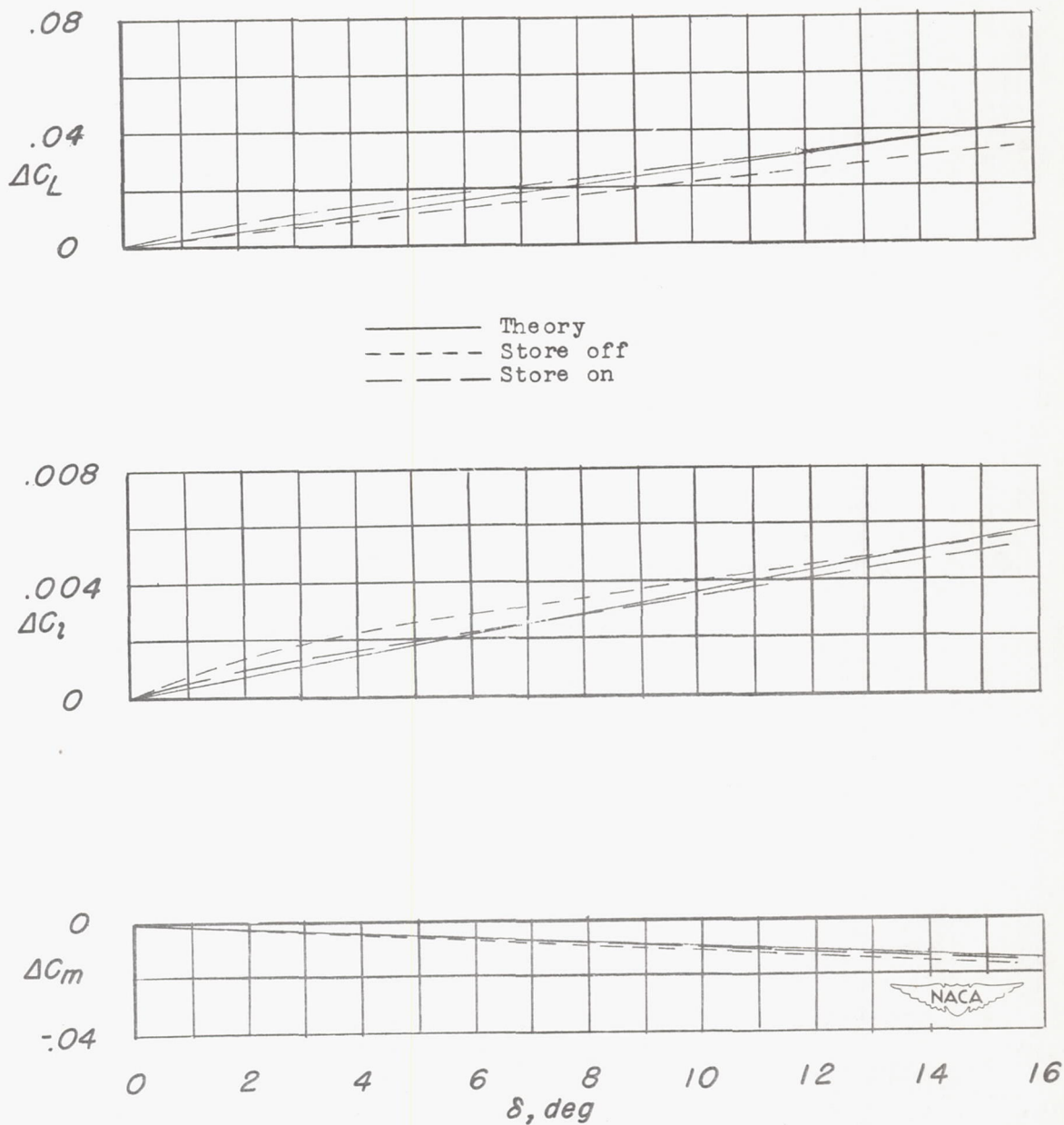


Figure 19.- Variation of the aerodynamic characteristics with control deflection of a tapered unswept wing with a 0.25c trailing-edge flap. External store off and on. $R = 2.3 \times 10^6$; $M = 1.90$; $\alpha = 0^\circ$.